Adult life strategy affects distribution patterns in abyssal isopods – implications for conservation in Pacific nodule areas

Saskia Brix[1], Karen J. Osborn[2], Stefanie Kaiser[1,3,4], Sarit B. Truskey[2], Sarah M. Schnurr[1,5], Nils Brenke[1], Marina Malyutina[5,6] & Pedro M. Martinez Arbizu[1,5]

[1]*Senckenberg am Meer, German Centre for Marine Biodiversity Research (DZMB) c/o Biocenter Grindel, Center of Natural History (CeNak), Universität Hamburg, Martin-Luther-King-Platz 3, 20146 Hamburg, Germany*

[2]*Smithsonian National Museum of Natural History, 10th and Constitution Ave NW, Washington, DC, 20013 USA*

[3]*CeNak, Center of Natural History, Universität Hamburg, Martin-Luther-King-Platz 3, 20146 Hamburg, Germany*

[4]*present address: University of Łódź, Department of Invertebrate Zoology and Hydrobiology, Banacha St. 12/16, Łódź, 90-237, Poland*

[5]*University of Oldenburg, FK V, IBU, AG Marine Biodiversitätsforschung, Ammerländer Heerstraße 114-118, 26129 Oldenburg*

[6] *A.V. Zhirmunsky National Scientific Center of Marine Biology, Far Eastern Branch, Russian Academy of Sciences, Palchevsky St, 17, Vladivostok 690041, Russia*

Correspondence to: Saskia Brix (sbrix@senckenberg.de)

Abstract

With increasing pressures to extract minerals from the deep seabed, understanding the ecological and evolutionary processes that limit the spatial distribution of species is critical to assessing ecosystem resilience to mining impacts. The aim of our study is to gain a better knowledge about the abyssal isopod crustacean fauna of the central Pacific manganese nodule province (Clarion Clipperton Fracture Zone, CCZ). In total, we examined 22 epibenthic sledge (EBS) samples taken at five abyssal areas located in the central northern Pacific including four contracting areas and one Area of Particular Environmental Interest (APEI3). Additional samples come from the DISCOL Area situated in the Peru Basin, south-eastern Pacific. Using an integrative approach that combined morphological and genetic methods with species delimitation analyses (SD) we assessed patterns of species range size, diversity and community composition for four different isopod families (Munnopsidae Lilljeborg, 1864; Desmosomatidae Sars, 1897; Haploniscidae Hansen, 1916 and Macrostylidae Hansen, 1916) displaying different dispersal

capacities as adults. Isopods are brooders, so their distribution and connectivity cannot be explained by larval dispersal, but rather by adult locomotion. In particular, our objectives were to 1) identify potential differences in the distributional ranges of isopod families relative to their locomotory potential, and to 2) evaluate the representativeness of the APEI for the preservation of regional biodiversity in the CCZ following mining disturbances. From 619 specimens, our SD analysis could distinguish 170 species, most of which were new to science (94.1%). We found that increased locomotory ability correlated with higher species diversity with nine species of Macrostylidae, 23 of Haploniscidae, 52 of Desmosomatidae and 86 of Munnopsidae. This is supported by family-level rarefaction analyses. As expected, we found the largest species ranges in the families with swimming abilities, with a maximum recorded species range of 5245 km and 4480 km in Munnopsidae and Desmosomatidae respectively. The less motile Haploniscidae and Macrostylidae had maximal species ranges of 1391 km and 1440 km respectively. Overall, rarefaction analyses indicated that species richness did not vary much between areas, but the real number of species was still not sufficiently sampled. This is also indicated by the large proportion of singletons (40.5%) found in this study. The investigated contractor areas in the CCZ were more similar in species composition and had a higher proportion of shared species between each other than the closely located APEI3 and the distantly located DISCOL Area. In fact, the DISCOL Area, located in the Peru Basin had more species in common with the core CCZ areas than APEI3. In this regard, APEI3 does not appear to be representative to serve as a reservoir for the fauna of the investigated contractor areas, at least in isopods, as it has a different species composition. Certainly, more data from other APEIs, as well as preservation reference zones within contractor areas, are urgently needed in order to assess their potential as resources of recolonization of impacted seabed.

1 Introduction

Spanning 60% of the Earth's surface, deep-sea areas (below 200 m water depth) harbor an immense diversity of habitats and species, but also large deposits of metal-rich seafloor minerals (e.g., polymetallic sulphides, cobalt-rich ferromangansese crusts, phosphorite- and polymetallic [Mn-] nodules). Despite the challenges to initial endeavors to explore these resources starting in the 1960s,

growing economic interests coupled with advancing technologies to extract minerals from the seafloor have now made deep-sea mining a reality (Wedding et al. 2015), but may become reality in the next years.

The abyssal Clarion Clipperton Fracture Zone (CCZ, Figure. 1), located in the tropical north-eastern Pacific is commercially the most important area for exploring Mn-nodule mining (in the CCZ it is one step further than prospection). Extraction of these mineral resources will inevitably lead to habitat loss and changes at the directly mined sites primarily through removal, blanketing and compaction of the upper sediment layer (5-20 cm) (Miljutin et al. 2011; Ramirez-Llodra et al. 2011; Jones et al. 2017; Gollner et al. 2017). Furthermore, areas beyond the actual mining block may be indirectly affected through the generation of a sediment cloud, as well as discharge water from dewatering processes at the sea surface (Oebius et al. 2001; Hauton et al. 2017). The impacts associated with deep-sea mining have already been outlined in earlier studies (e.g. Thiel and Forschungsverbund Tiefsee-Umweltschutz 2001). As part of their Environmental Management Plan (EMP), the International Seabed Authority (ISA) designated a network of nine of Areas of Particular Environmental Interest (APEIs) bordering the CCZ, where no mining takes place, to enable recovery of impacted populations and communities (Smith et al. 2008a; Wedding et al. 2013, 2015; Lodge et al. 2014). The prerequisite for these areas is that they are representative in terms of biodiversity and species composition and cover the entire spectrum of the habitat and community types available in the CCZ. However, data from APEIs, which have been very limited to date, bring into question their representativeness and suitability as a biodiversity reservoir (Vanreusel et al. 2016; Bonifacio et al. 2020; Christodoulou et al. 2020).

As mining will severely impact the communities along large swathes of the seafloor, recovery will only be possible through recolonization from surrounding areas. In order to make predictions on the recolonization potential of the deep-sea fauna, sound understanding of the modes and drivers of species' geographic distributions is required. That is, species with a broader distribution and better dispersal ability likely have a greater potential to recolonize impacted areas compared to species with narrower geographic ranges, which likely have an increased risk of local extinction following regional mining disturbance (Roberts & Hawkins 1999). In turn, this understanding would contribute to defining the extent and

location of ecological reserve areas in the CCZ (Baco et al. 2016; Vanreusel et al. 2016; De Smet et al. 2017).

In this study, we assess the role of adult lifestyle in determining the large-scale distribution of asellote isopods across the CCZ. Asellota of the superfamily Janiroidea are one of the most numerous and diverse crustacean taxon encountered within abyssal benthic samples (Brandt et al. 2007). With only a few exceptions, isopods lack planktonic larvae, and thus levels of gene flow result from the active and/or passive migration of adults (Brandt 1992). For these reasons, they have been frequently used as model organisms to study patterns of species range size and diversity in the deep sea (Hessler and Wilson 1983; Rex et al. 1993; Brandt 1995; Wilson 1998; Stuart et al. 2003; Brandt et al. 2007, 2012; Kaiser et al. 2007; Janssen et al. 2015; Wilson et al. 2017; Brix et al. 2018, Jennings et al. 2019). Asellotes are principally detritivores and foraminiferivores, but different groups show different lifestyles.

In this study, we chose four families along a spectrum of adult locomotion abilities, the Munnopsidae Lilljeborg, 1864, the Desmosomatidae Sars, 1897, the Haploniscidae Hansen, 1916 and the Macrostylidae Hansen, 1916 (Figure 2).

The Munnopsidae Lilljeborg 1864 are the most diverse and abundant janiroids in the deep sea and their diversity is reflected in numerous morphological and ecological adaptations, most important of which is their paddle-like posterior legs that are highly specialized for swimming or digging (Malyutina et al. 2020, Riehl et al. 2020). Some munnopsid species have moved towards a benthopelagic (e.g., in *Munnopsoides* Tattersall, 1905) or even holopelagic (e.g., in *Paramunnopsis* Hansen, 1916) mode, while others follow a burrowing (e.g., in *Ilyarachna* Sars 1869, or *Bellibos* Haugsness & Hessler, 1979), or epibenthic (e.g., in *Rectisura* Malyutina, 2003 or *Vanhoeffenura* Malyutina, 2004) life style (reviewed in Osborn 2009). In the Desmosomatidae, usually referred to as an epifaunal family, swimming adaptations are only poorly expressed compared to the Munnopsidae (Hessler 1981; Hessler and Stromberg, 1989). Yet, desmosomatids bear long natatory setae on their posterior pereopods and are thus considered to be moderate swimmers (Hessler 1981; Svarvasson 1984; Hessler and Strömberg, 1989; Brix et al., 2015, Bober et al. 2018). The Haploniscidae have no modifications for swimming or burrowing. While *in situ* observations are lacking, information from epibenthic sledge and core sampling suggests haploniscids

live at or near the sediment surface (Harrison 1989). Finally, the Macrostylidae, due to their infaunal tubicolous mode of life, are expected to have the least dispersal potential and thus the smallest distributional ranges. However, their sexual dimorphism may allow males of some lineages to be more mobile on the suprabenthos compared to the females (Harrison 1989; Hessler and Strömberg 1989; Riehl and Kaiser 2012; Bober et al. 2018).

In a previous molecular assessment of wide-spread isopod species across the Mid-Atlantic Ridge (MAR), Bober et al. (2018) found lifestyle to have a profound effect on dispersal distances, with munnopsid species maintaining gene flow across the MAR, while distributional ranges in desmosomatids, nannoniscids (Brix et al. 2018) and macrostylids were much more restricted (Riehl et al. 2017). Thus, we expect munnopsid species to exhibit the widest geographic distributions compared to other families. Furthermore, we expect to find the correlation between geographic distance and faunistic dissimilarity to be more pronounced in lineages with limited dispersal ability (Haye et al. 2012; Janssen et al. 2015; Riehl et al. 2018). In the absence of detailed information on species' distributional ranges in the CCZ, and the abyss in general, using lifestyle as a dispersal ability proxy may be useful in forecasting faunal recolonization potential following disturbance events and related environmental changes. Such proxies become useful for defining operational units for conservation planning due to their high richness of, unfortunately, largely undescribed isopod species.

In the course of the *Joint Programming Initiative Healthy and Productive Seas and Oceans (JPI Oceans) pilot action "Ecological aspects of deep-sea mining"*, sampling was conducted during the SO239 and SO242 expeditions in 2015 to obtain samples from contractor areas in the CCZ and APEI3 as well as the DISCOL Area in the Peru basin. From these samples, the isopod fauna has been examined. The primary objective of this study is two-fold: first, to identify potential differences in distributional ranges of four different deep-sea janiroid families with varying lifestyles (Munnopsidae, Desmosomatidae, Haploniscidae, and Macrostylidae) and in order to determine if these can be used as a surrogates to estimate dispersal distances. Second, to gain knowledge of the diverse species composition and connectivity of the core CCZ contractor areas in contrast to a closely located APEI and a distantly located Mn-nodule area DISCOL.

2 Material and Methods

2.1 Sampling and sample preparation

Samples were collected during two expeditions in the course of the JPI Oceans Pilot Action "Ecological Aspects of Deep-Sea Mining" (JPIO) to the CCZ and DISCOL Area in the north-eastern and south-eastern Pacific respectively (see cruise reports by Greinert 2015; Boetius 2015; Martinez Arbizu & Haeckel 2015; Figure 1). Within the CCZ, samples were collected from four different contacting areas from east to west: BGR (German contractor), IOM (Interoceanmetal Joint Organization), GSR (Belgian contractor), IFREMER (French contractor) and one APEI (APEI3: Area of Particular Environmental Interest number 3). Isopod specimens were collected with an epibenthic sledge (EBS) in the CCZ (SO239 cruise, 13 EBS deployments, Suppl. Table 1) and the Peru Basin (SO242-1 cruise, nine EBS deployments, Suppl. Table 1) from the RV *Sonne* in 2015.

Samples were immediately fixed on deck in pre-chilled 96% non-denatured ethanol and kept cool throughout the sorting process according to Riehl et al. (2014). One to three posterior legs (natapods) of each isopod specimen were dissected and used for DNA extraction. Before DNA extraction all isopod specimens were morphologically determined to family level and given individual voucher numbers. All voucher specimens will be stored at the Center of Natural History, Hamburg (CeNak) or the crustacean collection Senckenberg, Frankfurt after final species descriptions. Before being formally described, the isopod specimens are remaining in the DZMB storage. After DNA extraction, all isopod specimens were identified morphologically to species level using a LEICA MZ 12.5 stereomicroscope by SB, NB, and MM. All determinations were entered into the excel spreadsheet (Suppl. Table 1) using this as baseline for creating maps in QGIS, as well as for statistical analysis.

2.2 Data storage and handling

All specimen information and molecular data are managed via the Barcode of Life database (BoLD) in the projects “CCZ - Clarion and Clipperton Fracture Zones biodiversity” and “DISCOL - DISturbance and reCOLonization experiment in a manganese nodule area of the SE Pacific Ocean”. For this publication we created a dataset “Dataset - DS-LOCOM Locomotion of adult isopods influences

distribution" holding a subset of 619 specimens for GenBank submission and making the sequences visible after publication. All data are stored in the BoLD along with a project OECID, which contains all available data and is made publicly available via GenBank submission. The BIN system in BoLD compares newly submitted sequences with all already available sequences in BoLD clustering them according to their molecular divergence using clustering algorithms. Each cluster receives a unique BIN (barcode identity number as stated for each specimen with COI sequence in Table1).

2.3 Molecular Methods

We carried out a molecular analysis of two mitochondrial DNA markers (COI and 16S) backed up by morphological determinations, to delineate species in an integrative approach. Based on this species delimitation, we compared species richness and community composition of the different areas (APEI vs. contractor areas vs. DISCOL). A fragment of the mitochondrial gene Cytochrome Oxidase Subunit 1 (COI) was amplified and sequenced using the primers jgHCO2198 and jgLCO1490 (Geller et al., 2013) following the protocol of Riehl et al. (2014). Ribosomal 16S sequences were amplified and sequenced using the primers 16Sar and 16Sbr (Palumbi, 1992). The sequences were processed using Geneious 11.1.3 and compared against the GenBank nucleotide database. Sequences were aligned using MAAFT 7.388 (Katoh and Standley, 2013) implemented within Geneious v. 10.1.3. COI sequences were translated into amino-acid sequences within Geneious and checked for stop codons to prevent the inclusion of pseudogenes (Buhay, 2009). COI and 16S datasets were used individually for VSearch and ABGD species delimitation analyses and both individually and concatenated as a single mitochondrial dataset for phylogenetic tree reconstruction and PTP/mPTP species delimitation analyses. Tree estimations for each family were run in RAxML (Katoh and Standley, 2013) using the GTRGAMMA model and 1000 bootstrap replicates.

Outgroups for each family tree consisted of the following: Macrostylidae = *Thaumastosoma diva* KY951731, *Thaumastosoma platycarpus* IDesm10, *Ketosoma vemae* VTDes013 (16S only), KM14-Iso261 *Ketosoma* sp. 2, KY951731, and *Ketosoma hessleri* KY951729. Haploniscidae = *Ianiropsis epilittoralis* AF260835, AF260836, AF260858, and AF260859. Desmosomatids = *Betamorpha*

fusiformis EF116524, EF116525, EF116527, EF116528, and *Betamorpha africana* EF682292. Munnopsidae = *Thaumastosoma platycarpus* IDesm10, *Ketosoma vemae* VTDes013, *Ketosoma werneri* D3D60 (COI only), and *Thaumastosoma diva* D3D64 (16S only). Outgroups were chosen based on the most recent evidence for likely sister groups and available sequences.

2.4 Molecular species delimitation

Multiple species delimitation methods were applied to the four datasets and results varied based on the amount of within clade sampling, occurrence of singletons, and within and between clade variation. VSearch (Rognes et al., 2016) applies a pairwise identity threshold and generates clusters of sequences that fall within a specified percent identity, thus assuming a barcode gap, though these can be hard to identify in some cases. VSearch was performed on individual genes without an outgroup. ABGD was performed through the online ABGD webserver (http://wwwabi.snv.jussieu.fr/public/abgd/abgdweb.html, 08/18/2018; X = 0.5) on COI and 16S alignments by family. ABGD was performed on uncorrected p-distances using entire datasets under the assumption that the smallest gap in the pairwise distance histogram reflected the boundary between intraspecific variation (smaller values) and interspecific variation (larger values). Poisson tree processes (PTP) and multi-rate PTP were run using the stand alone mPTP software implementing -single and –multi switch commands on the fully bifurcated trees generated above. Our data contained multiple individuals with the same haplotypes, but the replicate haplotypes can confound delimitation analyses and lead to over-splitting (Marki et al., 2018), so we calculated the minimum branch length for each sequence and used the minimum branch threshold option in order to ignore these replicate branches in subsequent PTP/mPTP analyses. MCMC analyses were run for 100 million generations, sampling every 10,000 and discarding the first 2 million generations as burn-in. Analyses were initiated using a random delimitation as the starting point. We ran three MCMC chains for each analysis and assessed chain convergence by checking average standard deviation of delimitation support values (ASDDSV) across the three independent MCMC runs, accepting values near zero and below 0.05 as individual MCMC chains appearing to converge on the same distribution of delimitations (Ronquist et al., 2012, Kapli et al., 2017).

We inspected the MCMC output trees and collapsed all putative species clades that had support below 0.70, which resulted in the number of supported clades being within the credible range of delimited species (CCI) and the range across CCI where probability is 0.95 (HPD). The ML estimate, on the other hand, was not always within these intervals, meaning that this ML point estimate delimitation was not supported by MCMC analyses (the estimate may instead represent a local maximum or random solution derived across the ML likelihood surface) and demonstrates the importance of running MCMC analyses. Singletons greatly affected mPTP analyses but not PTP or ABGD, thus singletons were removed from mPTP and retained for PTP and ABGD.

2.5 Isopod Communities and diversity analyses

Analysis of community similarity between areas and their diversity was performed in R using the package 'vegan' (Oksanen et al 2008). The sampling effort, expressed as the number of EBS deployments per area was uneven, ranging from two to eight deployments per sampling area, therefore the similarity between communities was done using relative abundance (Chord distance, see Legendre and Gallagher 2001) and 'presence-absence' to explore faunistic differences. Ordination was done using nMDS. The community table (Suppl. Table 2) shows the number of specimens from each species found adding up all EBS samples for a given area. As the number of specimens found differs between areas, diversity comparison was achieved using rarefaction curves, together with standard diversity indices Shannon, Simpson and Jaccard's Evenness. The expected number of species per area was inferred using extrapolation methods. Chao1 (Chao 1994, Colwell and Coddington 1994) uses the proportions of singletons and doubletons in the sample to estimate expected species richness, while ACE (Chazdon et al 1998) is an abundance-based coverage estimator. For the analysis of beta (regional) diversity, the total multiple-site beta diversity β_{SOR} was calculated using the modified Sørensen Index (Sørensen 1948, Balseaga and Orme 2012), and β_{SOR} was decomposed into its additive components "multiple-site species turnover" β_{SIM} (Simpson Index, Simpson 1943) and "multiple-site nestedness" β_{SNE} using R package 'betapart' (Balseaga 2010, Balseaga and Orme 2012). In order to explore the relative contribution of every area to species turnover and nestedness, these values were calculated taking one area out each time in a

jackknife approach. Changes in turnover and nestedness are attributable to the area each time excluded from the analysis. UpSet Plots were done using R package UpSetR (Conway et al., 2017).

3 Results

3.1 Species Delimitation

All isopod families were reciprocally monophyletic (Figures 3-6). As expected with fast evolving genes such as COI and 16S, good resolution was given at the tips of the tree and most recent relationships such as species and sometimes even generic level, however, no resolution of relationships deeper in the trees was obtained. Given that the research question here is one of species delimitation, we did not attempt to find markers that would resolve deeper nodes in the trees.

It is notable that the percentage of species new to science was quite high, reaching 94.1% in our dataset. Of the ten described species, five were either described in the course of the JPIO sampling campaign or other CCZ and DISCOL collections (Malyutina & Wägele 2001; Malyutina 2011; Malyutina et al. 2020; Riehl & De Smet 2020). The remaining species, all belonging to the Munnopsidae, appear to have wide (pan-oceanic) distributions.

The congruent species delimitation resulted in 86 munnopsid species OTUs (Suppl. Table 1, Figure 3). Putative species clade definition based on genetic data suggested there was substantial cryptic diversity within the Munnopsidae. Specimens identified as belonging to *Disconectes* belonged to 14 different putative species, of which those putative species formed seven higher level clades. Specimens identified as belonging to the "catch-all" genus *Eurycope* belonged to 22 different putative species, of which those putative species formed nine higher level clades. One putative *Paramunnopsis* species was collected from three different regions, while another was collected from two different regions and was found to be within the same putative species clade as a specimen identified as *Munnopsis abyssalis*. Of the six putative *Betamorpha* species, four were singletons and one contained specimens collected from three different regions. All collected *Bellibos*, belonging to two putative species, were collected from a single region.

The congruent species delimitation resulted in 52 desmosomatid species OTUs (Suppl. Table 1, Figure 4). The genera *Chelator* Hessler, 1970 (6 spp.), *Oecidiobranchus* Hessler, 1970 (1 sp.), *Mirabilicoxa* Hessler, 1970 (12 spp.), *Eugerdella* (Kussakin, 1965) (18 spp.), *Disparella* Hessler, 1970 (5 spp.), *Prochelator* Hessler, 1970 (4 spp.) and *Eugerda* Meinert, 1895 (3 spp.) were present in our dataset. Genetically defined clade composition closely mirrored the morphological identification (Figure 4).

The congruent species delimitation resulted in 23 haploniscid species OTUs (Suppl. Table 1, Figure 5), which are all new to science The clades represent the genera *Mastigoniscus* (9 spp.), *Haploniscus* (9 spp.) and *Chauliodoniscus* (5 spp.).

The congruent species delimitation resulted in nine macrostylid species in this mongeneric family (Suppl. Table 1, Figure 6). Putative species "*Macrostylis* sp. 1", collected from both GC area and adjacent to IOM area, was strongly supported as sister to the rest of the available macrostylids. The remainder of the macrostylids formed a single clade that was differentiated into seven individual putative species clades (Figure 6). Only two of these putative species clades can be easily distinguished from the others based on morphology - while the rest have yet to have morphological apomorphies identified for them. All eight putative species clades were supported by a minimum bootstrap value of 97% in the maximum likelihood-based phylogenetic estimations. These nine species are the same that were stable across both COI/16S species delimitation analyses (Osborn et al. in prep. for detailed species delimitation analyses comparing methods and challenges with each family's dataset). It may be possible with additional sampling to separate the putative species further but based on this dataset, there was not consistent evidence for further splitting, so we chose to be conservative with regard to splitting putative species. Four species clades were geographically isolated within a single CCZ region (Figure 6, clades 4, 6, 7 and 8), the rest contained members from two to five regions. There was genetic signal that suggested genetic differentiation between regions within the largest putative species clade with representatives collected from five regions, but this differentiation, or perhaps our sample size, was not sufficient to support further species level splits.

3.2 Diversity Comparison by Family

The dataset comprised 619 specimens belonging to 170 putative genetic species (=OTUs) (Suppl. Table 1). Munnopsidae was represented in the whole dataset by 294 specimens (199 in CCZ) belonging to 86 species (71 in CCZ, 20 in DISCOL). Desmosomatidae was represented by 143 specimens (103 in CCZ) belonging to 52 species (42 in CCZ, 11 in DISCOL). Haploniscidae was represented by 88 specimens (53 in CCZ) belonging to 23 species (18 in CCZ, five in DISCOL). Macrostylidae was represented by 94 specimens (70 in CCZ) belonging to only nine species (seven in CCZ, two in DISCOL) (Table 3).

The rarefaction curves of the Munnopsidae and Desmosomatidiae showed no signs of saturation (Figure 7). This is supported by the Chao1, which predicted the expected number of Munnopsidae and Desmosomatidae species as 110 and 98 respectively (Table 3). In contrast, the curves of Haploniscidae and Macrostylidae approached saturation, a state also indicated by the predicted number of species by Chao1, which suggested that no additional (unseen) species of Haploniscidae and Macrostylidae were expected in the present dataset (Figure 7, Table 3).

Total beta diversity (βSOR) and species turnover (βSIM) increased in this sequence: Munnopsidae (βSOR = 0.873; βSIM = 0.860), Desmosomatidae (βSOR = 0.904; βSIM = 0.895) and Haploniscidae (βSOR = 0.916; βSIM = 0.898, Table 3). This pattern was not evident when comparing sites within the CCZ (Table 3). Macrostylidae had lower beta diversity and species turnover (βSOR = 0.809; βSIM = 0.777) mainly due to a single species that shows a large distribution range (see discussion).

3.3 Community and Diversity Comparison by Area

In total, we examined 22 EBS deployments taken from six abyssal areas. Sampling effort was uneven between sampling sites, with most samples taken in the DISCOL area of the Peru Basin (8). For all other areas 2–4 sites were sampled. None of the 170 species were recorded in all six areas. The most common species was *Macrostylis*_M05 with 46 specimens and was present in all areas besides DISCOL. Other species (see Appendix supplement 1) with ten or more specimens were the munnopsids: *Disconectes*_Mu11 (22 specimens), *Eurycope*_Mu37, *Disconectes*_Mu08 (both with 18 specimens), and *Munneurycope*_Mu67, the haploniscids: *Haploniscus*_H10 (13 specimens each) *Mastigoniscus*_H22

(with 12 specimens), the desmosomatid, *Eugerdella*_D39, and the macrostylids: *Macrostylis*_M03 and *Macrostylis*_M04 (with 10 specimens each). The remaining 177 species had less than ten specimens, 68 species were represented by singletons.

The total number of species found was relatively similar between sites ranging from 38 (GSR) to 50 species (IFREMER). Remarkably the number of species neither correlates with number of specimens (Pearson correlation 0.34, p=0.49), nor with number of sampling sites per area (Pearson correlation -0.02, p=0.95). IOM supported the highest number of unique species (species recorded only in one area) with 36 species (90 % of the species present in the area were unique), followed by DISCOL (31 species, 76% unique) and FC (IFREMER; 34 species 68% unique). All other areas had less unique species. The extrapolated number of species present per area ranged between 49 (GC: BGR) and 80 (BC: GSR) according to Chao1, and between 53 (GC: BGR) and 80 (FC: IFREMER) according to ACE, which Chao1 and ACE predicted between 50% and 12% of the species remained unrecorded. Diversity values (Shannon, Simpson and Jaccard) were similarly high in all areas, with the exception of low diversity values from the BGR area (evenness 0.88, Simpson 0.94, Shannon 3.34).

Half of the EBS deployments (11) were in the core CCZ area (all areas excluding APEI3 and DISCOL), but these accounted for two thirds of the specimens (425) and two thirds of the species (117) recorded, instead of the half that would be expected. A total of 99 species (84% of all species) were found exclusively in the CCZ area. Chao1 and ACE predicted 137–146 species for the CCZ and 235–252 species for all areas together. Rarefaction analysis (Figure 8) shows that all areas are similar in terms of species richness with the lowest curve at BGR (slightly lower diversity) and the highest at IOM. No curves show signs of having reached an asymptote (Figure 8).

Table 2 shows the faunistic similarity between areas. The greatest number of shared species were between CCZ areas. For instance, GSR shares 16 species with each of BGR and IOM areas, and 11 species with IFREMER, yet only four species with DISCOL and only two with APEI3 (Table 2).

The highest number of non-shared species is present in APEI3 (19 species) followed by DISCOL (17 species) and IFREMER (16 species) areas (Figure 10). The highest numbers of non-shared species (mean 80.4 ±4.3) are found between APEI3 and any other area, followed by DISCOL (mean 78.4 ±6.5, Table

2), although the t-test shows no significant difference between them (p=0.58). The lower panel of the upset plot depicts the connectivity network. Few species are shared between areas, 11 species were shared between two areas, seven species between three areas, three species between four areas and just one species is present in five areas. The least connected site is APEI3, sharing only four species with other areas, followed by DISCOL sharing five species. BGR and GSR were better connected, sharing 13 and 14 species with other areas respectively.

The Upset Plot (Figure 12) summarizes number of shared species between areas considering all taxa together as well as by taxa. The highest number of non-shared species is present in APEI3 (19 species) followed by DISCOL (17 species) and IFREMER (16 species) areas. The other CCZ contractor areas were more similar to each other having just eight or less non-shared species. The lower panel of the upset plot depicts the connectivity network. Only few species are shared between areas, 11 species are shared between two areas, seven species between three areas, three species between four areas and just one species is present in five areas. The less connected site is APEI3, sharing only three species with other areas, followed by DISCOL sharing five species. BGR and GSR area better connected sharing up to 14 species with other areas. Considering the Upset Plot by isopod family it becomes evident that there are less connections (shared species) between areas the less motile the family is, Munnopsidae and Desmosomatidae showing a diverse set of connections and Haploniscidae and Macrostylidae showing less connections (see below).

Total multi-site beta diversity was high (total βSOR 0.885, Table 1), meaning that the overall similarity between areas was low. The beta diversity between CCZ-only areas was lower (total βSOR 0.767) revealing slightly higher congruence between areas in the CCZ. In both cases the highest proportion of beta diversity is due to species turnover (βSIM) with only a small proportion accounting for nestedness (βSNE), but the nestedness proportion is 3 times greater within CCZ areas (βSNE = 0.021) than when considering all areas together (βSNE = 0.007). This is also evidenced by removing the areas one by one and calculating beta diversity with the reminding areas only. Removal of APEI3 and DISCOL results in the highest increase in nestedness (βSNE goes from 0.007 to 0.011), while the removal of any of the CCZ areas either does not change βSNE or it decreases up to βSNE = 0.004.

Community analysis using Chord distance was ordinated in an nMDS diagram (Figure 9), showing the more similar CCZ areas clustering together and the more different DISCOL and APEI3 distinctly apart from each other and from the CCZ areas. Not so evident is the pattern in the presence/absence ordination (Figure 10) because of the high dissimilarity between areas. The ordination is highly influenced by the number of unique species, highest at IOM, lowest at BGR along the y-axis and other areas spread along the x-axis. The box-plot (Figure 11) shows highest median presence/absence dissimilarity to other areas at APEI3, DISCOL and IFREMER areas. The boxplot shows that the median Chord distance of the area to any other areas is greater at APEI3 and DISCOL and smaller at any of the CCZ areas. Remarkably, core CCZ (IFREMER, IOM, GSR, and BGR) and APEI3/DISCOL areas were more similar within than between despite APEI3 and CCZ being much closer to CCZ than to DISCOL.

3.4 Range Size

Connectivity between areas differed between families (Table 4, Figure 12). No species of any family was present in all six study areas, and only one munnopsid and one macrostylid species were present in five areas (Table 4). In total 77% of the species were recorded just in a single area, 13.9% in two areas, 5.3% in three areas, 2.6% in four areas and 1% in five areas. A total of six (66.6%) out of nine species of Macrostylidae were recorded in a single area. The most widely distributed species of Desmosomatidae was present in all four CCZ areas. The proportion of species present in a single area varies between families and this proportion is the lowest within Munnopsidae, i.e. 75.8% occurred only in one area, and it is higher in Desmosomatidae (77.7%) and Haploniscidae (83%) this showing, that less motile families tend to have species with more restricted distributions

The Upset plots (Figure 12) illustrate the unique and shared diversity for the total dataset as well as for each family across sampling locations. The lower part of the plots represents the connectivity network for all species and by family. Each vertical line represents a set of sites with shared species and the vertical bars represent how many species are shared in each combination. While Macrostylidae and Haploniscidae show only three and fourset of sites with shared species, the connectivity network is more

complex for Desmosomatidae and Munnopsidae with 11 and 17 sets respectively. The complexity of the connectivity network increases with increasing locomotory ability of the family.

Species ranges by family are summarized in Table 5. Ranges were calculated after excluding singletons. A total of 60 species of munnopsids, 29 desmosomatids, 19 haploniscids and eight of macrostylids were represented by more than one specimen in the dataset. The maximum distribution range was higher for the natatory families Munnopsidae and Desmosomatidae, 5245 km and 4480 km respectively. The less motile families Haploniscidae and Macrostylidae had maximun ranges of 1391 km and 1440 km respectively. The minimum ranges per family also correlated with locomotory ability being for Munnopsidae 253 km, for Desmosomatidae 40 km, for Haploniscidae 1 km and for Macrostylidae 130 m (Table 5).

4. Discussion

4.2 Lifestyle of adults determines species' distributional ranges

Presumed low levels of environmental variability and absence of obvious dispersal barriers, led to the assumption that deep-sea species have wider horizontal distributions compared to shallow-water representatives (McClain & Hardy 2010). However, molecular studies have shown that morphologically similar, but genetically distinct (cryptic) species are common among deep-sea lineages, fundamentally changing our understandings of deep-sea species distributions (e.g. Vrijenhoek et al. 1994; Pfenninger & Schwenk 2007; Raupach et al. 2007; Havermans et al. 2013; Brix et al. 2014, 2015; Jennings et al. 2018, 2019). Conversely, for some species there is morphological and genetic support for wide geographic distributions even across major topographic barriers (Brix et al. 2011; Menzel et al. 2011; Riehl & Kaiser 2012; Janssen et al. 2015; Easton & Thistle 2016; Bober et al. 2018; Brix et al.2018, Christodoulou et al. 2020). However, biological data on dispersal distances of deep-sea species are still fragmentary due to the low sampling effort compared to the sheer area of deep-sea floor, and the scant knowledge of species' taxonomy. The large proportion of new species commonly found in deep-sea environments (Brandt et al. 2007, Brix et al. 2018, Jennings et al. 2019, Kaiser et al. 2017), also seen in our dataset (Figures 3-6),

remains a major impediment to the understanding of large-scale distributional patterns. With our species delimitation analysis accompanied by morphological assessment, however, we provided a stable system for defining a species in the deep sea as the basis for a more detailed ecological examination of the samples.

Our results indicated, that life-style, and more precisely the locomotory (dispersal) capabilities of adult deep-sea asellotes are structuring their biodiversity patterns at medium and large scales. In-line with our hypothesis, we found species within the family Munnopsidae exhibited the widest geographic ranges among the four families examined (Table 5). The second most mobile family was the Desmosomatidae, who live on the surface of the sediments, but have posterior appendages modified for swimming, though not as pronounced as in the Munnopsidae. In contrast, there is no evidence that Haploniscidae can swim. These asellotes live on or in the sediments and have short walking legs that they use for crawling. Macrostylidae are assumed to likely live in tubes in the sediment, although some males of this family are good swimmers (Riehl et al. 2020).

Brandt et al. (2011) considered the influence of locomotion (mobility types) for the distribution of isopod families, but the study by Bober et al. (2018) is the only other known analysis to assess distributional ranges in abyssal isopods relative to locomotive capacity using molecular markers. Bober et al. (2018) compared differences in the dispersal capacity of species in four isopod families (Munnopsidae, Desmosomatidae, Nannoniscidae and Macrostylidae), which were collected along the Vema fracture zone and found on both sides of the MAR. Although their study was based on only a few model species, they could see patterns like those in our analysis. For example, Bober et al. (2018) were able to detect the same haplotypes across the MAR in the swimming munnopsid *Acanthocope galathea* Wolff, 1962. The molecular analysis of *A. galathea* samples from the Vema Facture Zone and CCZ confirmed a pan-oceanic distribution in this species (Bober, pers. Communication). By contrast, for the non-swimming Macrostylidae and weakly-swimming Desmosomatidae and Nannoniscidae, the MAR seemed to be a dispersal barrier (Bober et al. 2008). Notably, in their analysis two species of Macrostylidae and Desmosomatidae each crossed the MAR, but there was no evidence of genetic exchange. Using data from the same sampling campaign, Brix et al. (2018) showed that even robustly-

460 sampled species within Nannoniscidae and Desmosomatidae exhibit “small” ranges of around 500 km, and only three species were distributed in the order of 1,000–2,500 km. But we need to take into account that species ranges are biased by the sampling design and that there is a higher probability of sampling an abundant species than a widely distributed but rare species.

Although larval dispersal does not apply to isopods, since they brood their young, we would like
465 to point out, that most of the isopod species reported here are very small, in the range of few millimeters as adult. In this size range it is clear that also adult isopods will be transported by bottom currents, once they swim just a few centimeters above the bottom. Etter and Bower (2015) tested the distribution distance of planktonic larvae in the North Atlantic Ocean using physical particles as models. Their experiment showed that dispersal over hundreds of kilometers and even through current systems with a strong
470 temperature gradient is possible. Pelagic species and pelagic life stages of many benthic species can drift and swim across and/or between oceans during their lifetime. Fully benthic species, on the other hand, spend most of their life on or in the seabed, and thus may be dispersing over much shorter distances (Costello et al. 2017). Actively swimming taxa, such as the Munnopsidae that can swim 10s to 1000s of meters above the bottom, sometimes show a broad distribution that is less influenced by local water
475 masses (Schnurr et al. 2014, 2018). For other asellote families in the present dataset, local and regional bottom currents are likely to play a major role in shaping their distribution patterns (Riehl et al. 2018; S. Kaiser pers. communication).

Macrostylidae deserves a special mention. Species within this family had a remarkably narrow distribution range, as six out of nine species were found in a single area and two species in two contiguous
480 areas (Table 4). This pattern would have reinforced our hypothesis, except that one of the species (“sp. M”, OTU M04-M07, see Suppl. Table 1, Figure 6) is present in five areas. In our study, low morphological variation is contrasted by genetic differentiation in *Macrostylis* sp. M (cf. *metallicola*), which belongs to at least three different species according to our SD (Figure 6). If a real identification as *M. metallicola* can be provided for clade 5, this would follow the wide distribution of this species across
485 the CCZ according to Riehl and De Smet (2020). These authors stated that they found molecular hints of *M. metallicola* being a complex of more (cryptic) species and thus, the morphologically uniform

appearance leads to underestimating biodiversity or possibly the population is in the early stages of a radiation. Either way, mining would disrupt this evolutionary process and limit the genetic potential of the population and thus, cause changes in the radiation and distribution pattern of this species complex. The wide distribution of species M05 would have been easily explained if the males had shown a strong sexual dimorphism, but this was not the case in the individuals collected here.

A change to a more epifaunal or even swimming lifestyle in sexually mature males that mate with likely stationary females was discussed in species descriptions of strongly sexual dimorphic species such as those belonging to the Macrostylidae (Bober et al. 2017; Kniesz et al. 2017). Sex-specific differences in dispersal capacities are known more from Macrostylidae than from Munnopsidae, for which there are no documented dispersal-effecting sexual dimorphisms. In desmosomatid and haploniscids, sexual dimorphism is more pronounced than in munnopsids, in that males show more adaptations to swimming than females in various species. For example, the species delimitation done on the KuramBio II dataset for desmosomatids and nannoniscids (Jennings et al. 2020) revealed that a strong sexual dimorphism, especially in the genus *Mirabilicoxa*, limits morphological species determination and only the integrated approach combining genetics and morphology made a clear assignment to species possible.

We found both wide-ranging species and many singletons or species that occurred in a single area, especially within the Munnopsidae (Figure 3). Rarity like this, is a widespread phenomenon in deep-sea ecosystems (Brandt et al. 2007; Connolly et al. 2014). The high number of singletons in our dataset (Supplementary Table 1) may reflect the always insufficient sampling effort of deep-sea studies (Kaiser et al. 2007; Janssen et al. 2015). This interpretation is further supported by the rarefaction curves that show no asymptote, suggesting incomplete sampling of the isopod biodiversity in the region (Figure 8). Kaiser et al. (unpublished data) examined the phylogeographic structure in a genus of poorly dispersing nannoniscid isopods from the CCZ and found similarly contrasting distribution patterns. Some species show a wide geographic distribution (>1400 km), while other species show evidence of restricted distributions or limited species ranges. These authors found that isolation by distance seemed to explain the distribution patterns to some extent, but the degree of habitat heterogeneity and oceanographic currents were equally important.

4.4 APEIs are similar in diversity but not in species composition compared to contractor areas

Mining will fundamentally change the structure and function of resident communities and ecosystems. Thus, the implementation of set-aside areas, which remain untouched, can facilitate recolonization of impacted seafloor from external source populations (Cuvelier et al. 2018). Initially, a network of APEIs were defined on the basis of large-scale hydrographic and bathymetric features, incl. nodule densities, carbon flux and seamount distribution (Wedding et al. 2013). Furthermore, assumed dispersal distances of species were considered to promote population persistence. Until 2015, however, no biological sample was taken from any APEI in order to assess its suitability as a biodiversity reservoir. Only in the course of the MiningImpact and Abyssline projects, were the first samples collected from APEIs No. 3 and 6 (Amon et al. 2016, Martinez & Haeckel 2015). Published data on a number of fauna groups based on these samples indicate little resemblance between APEI3 communities and the contractor areas studied (Vanreusel et al. 2016; Jakiel et al. 2019; Bonifacio et al. 2020, Christodoulou et al. 2020). Bonifacio et al. (2020), for instance, investigated polychaete communities from the same sampling campaign as ours, and found considerably lower densities, diversity and similarity in species composition of APEI3 relative to contractor areas. Data on tanaidaceans from APEI3 also showed relatively low densities and species richness (Jakiel et al. 2019; Blazewicz et al. 2019). Further, Jakiel et al. (2019) found that only one-third of CCZ pseudotanaid richness was present in the APEI3. Christodoulou et al. (2020) studied the brittle stars in the CCZ, APEI3 and DISCOL and similar to the present study, they showed a greater faunistic similarity between core CCZ contractor areas than to other areas. In addition, the similarity of the core CCZ area was greater to the most distant DISCOL area that to the relatively close APEI3. For isopods in our study, diversity levels perceived from APEI3 were similar to the contractor areas (Table 1), but species composition was different with only a few shared species (Table 2). This supports the idea, that distance is not the only factor determining community similarity between areas. Christodoulou et al. (2020) suggest marked differences in POC-flux as a possible structuring factor. The APEI3 is located in an area with very low surface productivity compared to the core CCZ areas and the DISCOL region. Environmental conditions have been shown to differ significantly in the APEI3

compared to areas in the CCZ, notably lower POC fluxes to the seafloor, lower total organic carbon (TOC) content, as well as lower clay content (Volz et al. 2018). These differences likely explain the observed community differences (Blazewicz et al. 2019; Bonifacio et al. 2020, Christodoulou et al. 2020). In a study of Icelandic isopods, Brix et al. (2018), TOC and mud content were shown to be the main explanatory variables for variation in distribution of families, with different lifestyles (e.g., in-, vs. epi., vs. suprafauna) and thus likely differential use of food resources and substrate associations.

The CCZ is delimited to the north by the Clarion Fracture Zone (Hall and Gurnis, 2005). Bonifacio et al. (2020) argue that the latter limits dispersal between peripheral APEIs and CCZ contractor areas, at least for some taxa, similar to what was seen for the MAR (Bober et al. 2018; Guggolz et al. 2018; Riehl et al. 2018). As previously discussed, Bober et al. (2018) found highly mobile munnopsids were able to cross the MAR, while the distribution of species in more poorly dispersing taxa, such as the Desmosomatidae, Nannoniscidaea and Macrostylidae, was restricted. Similarly, our study showed the swimming families Munnopsidae and Desmosomatidae have little similarity between APEI3 and contractor areas. Therefore, we believe that other factors like contrasting food supply rather than physical barriers, shape the standing stocks of these species.

Taboada et al. (2018) investigated microsatellite data of a common demosponge species (*Plenaster craigi* Lim & Wiklund, 2017) with a limited dispersal capacity from three contractor areas (UK-1A, UK-1B and OMS) of the CCZ and APEI6. Their data revealed higher connectivity of distant populations (~800 km apart) compared to those only 10s of km apart. This unexpected pattern was attributed to hydrodynamic conditions on a small and larger scale, which on the one hand facilitates species dispersal over large distances, but locally may interrupt gene flow between populations (Taboada et al. 2018). Although they found evidence of genetic connectivity between UK-1A and APEI6 (which is located closely, to the UK-1A area) in *P. craigi*, they concluded that APEI6 alone does not appear to adequately preserve the genetic diversity of *P. craigi* in the region. At this stage more data from the remaining APEIs, particularly those situated to the south, are required to further assess the appropriateness of APEIs for conservation purposes, particularly in terms of representative environmental conditions, fauna, and overall size of these reserves. Together, these studies suggest that APEIs are inappropriate or

insufficient to capture the biodiversity of the CCZThe aim should therefore be to re-evaluate the suitability of the APEIs for the re-colonization of the proposed mining areas (Vanreusel et al. 2016; Blazewicz et al. 2019; Jakiel et al. 2019; Taboada et al. 2018, this study).

4.5 Implications for Conservation

Small-sized meio- and macrofaunal invertebrates, such as isopods make up a large proportion of CCZ diversity. Thus, especially for these small-sized faunal elements, studies on species richness and distribution patterns are needed for the development of management strategies for the preservation of abyssal biodiversity (Blazewicz et al. 2019). The widespread distribution of many munnopsid species suggests that at least some species may be able to recolonize affected areas, provided that the integrity of the habitat is restored. However, some species, like the Macrostylidae and some Haploniscidae are limited in their distribution, having been found in just one of the contractor areas. Therefore, their local loss may thus become a global loss. But even for widely distributed species, extinction of connecting population may result in loss of genetic diversity and recovery potential (Riehl and De Smet 2020). Janssen et al. (2019) stated that in the case of polychaetes with long- and short-distance dispersal capabilities, large populations are continuously distributed over large geographic scales. Although Janssen et al. (2019) suggested a similar pattern in isopods, they showed spatial genetic structuring of isopod populations did imply weak barriers to gene flow. They concluded that mining-related habitat destruction will most likely impact the continuity of isopod populations more severely than for other groups such as polychaetes. As a result of this study we can add that not all isopod families will be equally affected. Less motile families will be more severely affected. This assumes that ecosystem recovery after major impacts is predicted to occur slowly at evolutionary time scales. Haffert et al. (2020) calculated that the recovery of the biochemical fluxes in the upper centimeters of abyssal sediments after mining will take over 200 years.

Most species in our study are new to science or undescribed, and with increasing species accumulation curves, we are far from knowing how many isopod species live in the CCZ and how widespread they are. Our study of a community where over 94% of the isopod species are new to science or described within the last two years, indicates the need for quick assessment tools like molecular species

595 delimitation in the deep-sea environment. Additionally, taxonomic expertise is needed, which can lead to a description of the key species even though it is not possible to describe every single species (Brix et al. 2018). In addition, the exchange of images and sample sketches of species provided by taxonomist would contribute to taxonomic standardization between contractor areas and thus improve and refine biodiversity and biogeographic patterns.

600 We have been able to show, that less motile families of Isopoda, have more restricted distribution ranges. This has direct implications for recovery after mining operations. For these families, recolonization will need to start from nearby non-impacted areas. It is unlikely that pristine areas located far away from the mining operations will act as source-populations because they will most probably harbor a different set of species. The considerable differences we found between isopod communities of 605 APEI3 and contractor areas cause doubts of the representativity of APEIs for conserving biodiversity in the CCZ as a whole. However, our study has the obvious limitation that we have sampled only contractor areas located in the eastern CCZ and we have sampled only one APEI. Therefore, more data from other APEIs are urgently needed to assess the diversity and composition of their communities and the degree of faunal connectivity, which must lead to a new assessment and revision of protected areas for the CCZ. 610 We strongly suggest a declaration of APEIs within the core CCZ region as clear strategy to protect a more similar fauna to the areas that will be affected by mining.

Author contributions

Saskia Brix: Manuscript writing, coordination and management of sequence data (in BoLD), quality 615 check, morphological identification, discussing the species delimitations, figures and manuscript writing, preparing the voucher specimens for museum storage.

Karen J. Osborn: Data quality assessment/control, alignments, supervision of species delimitation analyses, tree/species delimitation figures, portions to the manuscript, editing.

Sarah Schnurr: preparing specimens for genetics and sampling on board as well as lab work at the Smithsonian producing the raw data and providing preliminary trees.

Sarit B. Truskey: performing the species delimitation and phylogenetic analyses and preliminary trees.

Stefanie Kaiser: manuscript writing, sorting and preparing specimens on board, helping with the morphological species delimitation

Nils Brenke: species determination of DISCOL Isopoda and morphological comparison to the JPIO dataset together with Saskia Brix.

Marina Malyutina: Identification of the Munnopsidae and linking the manuscript to the description of a new genus.

Pedro Martinez Arbizu: Paper idea and statistical analyses, manuscript writing and statistical figures.

Sample availability

No geoscientific samples which are registered as International Geo Sample Number (IGSN) have been used for the manuscript.

Competing interests

The authors declare that they have no conflict of interest.

Acknowledgements

Magdalini Christoudolu is thanked for helping with the BoLD management of the whole pacific project from which we extracted our dataset. Nele Johanssen and Torben Riehl gave us a first impression on the morphological determination of JPIO haploniscids and macrostylids. Karen Jeskulke not only helped with the lab work at the Smithsonian and the DZMB in Hamburg, she contributed largely to the databank entries at DZMB HH. SK acknowledges a grant from the German Academic Exchange Service (DAAD) and the Narodowa Agencja Wymiany Akademickiej (Poland) under the ULAM program. The cruises SO239 and SO242 were financed by the German Ministry of Education and Science (BMBF) as a

contribution to the European project JPI Oceans ‘‘Ecological Aspects of Deep-Sea Mining’’. The authors acknowledge funding from BMBF under Contract 03F0707E. This is publication number 72 from Senckenberg am Meer Metabarcoding and Molecular Laboratory.

References

Baco, A. R., Etter, R. J., Ribeiro, P. A., Von der Heyden, S., Beerli, P., & Kinlan, B. P.: A synthesis of genetic connectivity in deep-sea fauna and implications for marine reserve design. Mol Ecol, 25(14), 3276-3298, 2016.

Błażewicz, M., Jóźwiak, P., Menot, L., & Pabis, K.: High species richness and unique composition of the tanaidacean communities associated with five areas in the Pacific polymetallic nodule fields. ProOce, 102141, 2019.

Baselga, A.: Partitioning the turnover and nestedness components of beta diversity, Glob. Ecol. Biogeogr., 19, 134–143, https://doi.org/10.1111/j.1466-8238.2009.00490.x, 2010.

Balseaga, A., and Orme, C. D. L.: betapart: an R package for the study of beta diversity, Methods Ecol. Evol., 3, 808–812, https://doi.org/10.1111/j.2041-210X.2012.00224.x, 2012.

Bober, S., Riehl, T., Henne, S., Brandt, A.: New Macrostylidae (Isopoda) from the Northwest Pacific Basin decribed by means of integrative taxonomy with reference to geographical barriers in the abyss. Zool J of Linn Soc. 182(3). DOI: 10.1093/zoolinnean/zlx042, 2017.

Bober, S., Brix, S., Riehl, T., Schwentner, M., Brandt, A.: Does the Mid-Atlantic Ridge affect the distribution of abyssal benthic crustaceans across the Atlantic Ocean? Deep Sea Res Part II, 2018.

Brandt, A.: Origin of Antarctic Isopoda (Crustacea, Malacostraca). Mar. Biol. 113: 415. https://doi.org/10.1007/BF00349167, 1992.

Brandt, A., Brix, S., Brökeland, W., Choudhury, M., Kaiser, S., Malyutina, M.: Deep-sea isopod biodiversity, distribution and endemism in the Atlantic sector of the Southern Ocean – results from the ANDEEP I - III expeditions. Deep -Sea Res. II 54, 1760–1775, 2007.

Brandt, A., Bathmann, U., Brix, S., Cisewski, B., Flores, H., Göcke, C., Janussen, D., Krägefsky, S., Kruse, S., Leach, H., Linse, K., Pakhomov, E., Peeken, I., Riehl, T., Sauter, E., Sachs, O., Schüller, M., Schrödl, M., Schwabe, E., Strass, V., vanFraneker, J. A., Wilmsen, E.: Maud Rise–a snapshot through the water column. Deep-Sea Res, doi:10.1016/j.dsr2.2011.01.008, 2011.

Brix, S., Leese, F., Riehl, T., Kihara, T.C.: A new genus and new species of Desmosomatidae Sars, 1897 (Isopoda) from the eastern South Atlantic abyss described by means of integrative taxonomy. Mar Biodiv 45(1), 7–61, 2015.

Brix, S., Leese, F., Svavarsson, J.: A multi−gene analysis reveals multiple highly divergent lineages of the isopod Chelator insignis (Hansen, 1916) south of Iceland. Pol Pol Res 35(2), 225–242, doi: 10.2478/popore−2014−0015, 2014.

Brix, S., Riehl, T., Leese, F.: First genetic data for species of the genus *Haploniscus* Richardson, 1908 (Isopoda: Asellota: Haploniscidae) from neighbouring deep-sea basins in the South Atlantic. Zootaxa 2838, 79–84, 2011.

Brix, S., Bober, S., Tschesche, C., Kihara, T. C., Driskell, A., Jennings, R. M.: Molecular species delimitation and its implications for species descriptions using desmosomatid and nannoniscid isopods from the VEMA fracture zone as example taxa. Deep Sea Res II, 2018.

Brökeland, W.: Redescription of *Haploniscus rostratus* (Menzies, 1962) (Crustacea: Peracarida: Isopoda) with observations on the postmarsupial development, size ranges and distribution. Zootaxa, 2521, 1–25, 2010a.

Brökeland, W.: Description of four new species from the *Haploniscus unicornis* Menzies, 1956 complex (Isopoda: Asellota: Haploniscidae). Zootaxa, 2536, 1–35, 2010b.

Boetius, A., ed. (2015) RV SONNE Fahrtbericht / Cruise Report SO242-2: JPI OCEANS Ecological Aspects of Deep-Sea Mining, DISCOL Revisited, Guayaquil - Guayaquil (Equador), 28.08.-01.10.2015, GEOMAR Report, N. Ser. 027. GEOMAR Helmholtz-Zentrum für Ozeanforschung, Kiel, Germany, 552 pp., doi:10.3289/GEOMAR_REP_NS_27_2015.

Buhay, J. E.: “COI-like” Sequences Are Becoming Problematic in Molecular Systematic and DNA Barcoding Studies. J.of Crust. Biol., 29 (1,) 96–110, https://doi.org/10.1651/08-3020.1, 2009.

Cardoso, P., Erwin, T. L., Borges, P. A. V., New, T. R.: The seven impediments in invertebrate conservation and how to overcome them. Biol. Conserv. 144, 2647–2655, 2011.

Carney, R. C.: Oceanography and Marine Biology: An Annual Review. In: Zonation of deep biota on continental margins. Eds. R. N. Gibson, R. J. A. Atkinson, J. D. M. Gordon, Taylor & Francis, 211-278, 2005.

Chao, A.: Non-parametric estimation of the number of classes in a population, Scand. J. Stat. 11, 265–270, 1984.

Chazdon, R. L., Colwell, R. K., Denslow, J. S., Guariguata, M. R.: Statistical methods for estimating species richness of woody regeneration in primary and secondary rain forests of NE Costa Rica, in: Forest biodiversity research, monitoring and modeling: Conceptual background and Old World case studies, edited by: Dallmeier, F., and Comiskey, J. A., Parthenon Publishing, Paris, France, 285–309, 1998.

Christodoulou, M., O´ Hara, T, Khodami, S., Rodrigues, C.F., Hilario, A., Vink, A. & Martinez Arbizu, P.: Unexpected high abyssal ophiuroid diversity in polymetallic nodule fields of the Northeast Pacific Ocean, and implications for conservation. Biogeosciences, 17, 1845–1876, https://doi.org/10.5194/bg-17-1845-2020, 2020.

Colwell, R. K., Coddington, J. A.: Estimating terrestrial biodiversity through extrapolation. Phil. Trans. R. Soc. Lond. B, 345, 101–118, https://doi.org/10.1098/rstb.1994.0091, 1994.

Connolly, S. R., MacNeil, M. A., Caley, M. J., Knowlton, N., Cripps, E., Hisano, M., ... & Brandt, A. Commonness and rarity in the marine biosphere. *Proceedings of the National Academy of Sciences*, *111*(23), 8524-8529, 2014.

Conway, J.R., Lex, A. & N. Gehlenborg: UpSetR: an R package for the visualization of intersecting sets and their properties. Bioinformatics, 33 (18): 2938–2940, https://doi.org/10.1093/bioinformatics/btx364, 2017.

Costello, M. J., Chaudhary, C.: Marine Biodiversity, Biogeography, Deep-Sea Gradients, and Conservation,Current Biology, 27 (11) R511-R527,https://doi.org/10.1016/j.cub.2017.04.060, 2017.

De Smet, B., Pape, E., Riehl, T., Bonifácio, P., Colson, L., Vanreusel, A.: The Community Structure of Deep-Sea Macrofauna Associated with Polymetallic Nodules in the Eastern Part of the Clarion-Clipperton Fracture Zone. Front. Mar. Sci. 4:103. doi: 10.3389/fmars.2017.00103, 2017.

Easton, E. E., Thistle, D.: Do some deep-sea, sediment-dwelling species of harpacticoid copepods have 1000-km-scale range sizes? Mol. Ecol., 25(17), 4301-4318, 2016.

Etter, R. J., Bower, A. S.: Dispersal and population connectivity in the deep North Atlantic estimated from physical transport processes, DSR I: Oceanographic Research Papers, Volume 104, 159-172, https://doi.org/10.1016/j.dsr.2015.06.009, 2015.

Fiser, C., Robinson, C., Malard, F.: Cryptic species as a window into the paradigm shift of the species concept. Mol. Ecol., 27, 613-635, 2017.

Fontaneto, D., Flot, J.-F., Tang, C. Q.: Guidelines for DNA taxonomy, with a focus on the meiofauna. Mar. Biodivers. 1–19, doi:10.1007/s12526-015-0319-7, 2015.

Fujita, M. K., Leaché, A. D., Burbrink, F. T., McGuire, J. A., Moritz, C.: Coalescent-based species delimitation in an integrative taxonomy. Trends Ecol. Evol. 27, 480–488, 2012.

Geller, J., Meyer, C., Parker, M., Hawk, H.: 2013 Redesign of PCR primers for mitochondrial cytochrome c oxidase subunit I for marine invertebrates and application in all-taxa biotic surveys. Mol. Ecol. Res., https://doi.org/10.1111/1755-0998.12138, 2013.

Grantham, B. A., Eckert, G. L., Shanks, A. L.: Dispersal potential of marine invertebrates in diverse habitats. Ecol Appl 13: 108–116, 2003.

Greinert, J., ed. (2015) RV SONNE Fahrtbericht / Cruise Report SO242-1: JPI OCEANS Ecological Aspects of Deep-Sea Mining, DISCOL Revisited, Guayaquil - Guayaquil (Equador), 28.07.-25.08.2015, GEOMAR Report, N. Ser. 026. GEOMAR Helmholtz-Zentrum für Ozeanforschung, Kiel, Germany, 290 pp., doi:10.3289/GEOMAR_REP_NS_26_2015

Gollner, S., Kaiser, S., Menzel, L., Jones, D. O., Brown, A., Mestre, N. C., Cuvelier, D.: Resilience of benthic deep-sea fauna to mining activities. Mar. Env. Res., 129, 76-101, 2017.

Haffert, L., Haeckel, M. de Stigter, H. & Janssen, F.: Assessing the temporal scale of deep-sea mining impacts on sediment biogeochemistry. Biogeosciences, 17, 2767–2789, https://doi.org/10.5194/bg-17-2767-2020, 2020.

Hall, C. E. and Gurnis, M.: Strength of fracture zones from their bathymetric and gravitational evolution, J. Geophys. Res.-Sol. Ea., 110, B01402, https://doi.org/10.1029/2004JB003312, 2005.

Harrison, K.: Are deep-sea asellote isopods infaunal or epifaunal?. Crustaceana, 56(3), 317-319, 1986.

Haye, P. A., Varela, A, Thiel, M.: Genetic signatures of rafting dispersal in algal-dwelling brooders *Limnoria* spp. (Isopoda) along the SE Pacific (Chile). Mar. Ecol. Prog. Ser., 455, 111–122. https://doi.org/10.3354/meps09673, 2012.

Hauton, C., Brown, A., Thatje, S., Mestre, N. C., Bebianno, M. J., Martins, I., Bettencourt, R., Canals, M., Sanchez-Vidal, A., Shillito, B., Ravaux, J., Zbinden, M., Duperron, S., Mevenkamp, L., Vanreusel, A., Gambi, C., Dell'Anno, A., Danovaro, R., Gunn, V., Weaver, P.: Identifying Toxic Impacts of Metals Potentially Released during Deep-Sea Mining—A Synthesis of the Challenges to Quantifying Risk. Front. Mar. Sci. 4, 368. doi: 10.3389/fmars.2017.00368, 2017.

Havermans, C., Sonet, G., d'Acoz, C. U., Nagy, Z. T., Martin, P., Riehl, T., Brix, S.: Genetic and Morphological Divergences in the Cosmopolitan Deep-Sea Amphipod *Eurythenes gryllus* reveal a Diverse Abyss and a Bipolar Species. PLoS One, 2013.

Hessler, R.R.: The Desmosomatidae (Isopoda, Asellota) of the Gay Head-Bermuda transect. Bull. Scripps Inst. Oceanogr. 15, 1–185, 1970.

Hessler R.R.: Evolution of Arthropod Locomotion: A Crustacean Model. In: Herreid C.F., Fourtner C.R. (eds) Locomotion and Energetics in Arthropods. Springer, Boston, MA, 1981.

Hessler, R. R., Strömberg, J.-O.: Behavior of janiroidean isopods (Asellota), with special reference to deep-sea genera, Sarsia, 74:3, 145-159, DOI: 10.1080/00364827.1989.10413424, 1989.

Hilário, A., Metaxas, A., Gaudron, S. M., Howell, K. L., Mercier, A., Mestre, N. C., Young, C.: Estimating dispersal distance in the deep sea: challenges and applications to marine reserves. Frontiers in Marine Science, 2, 6, 2015.

Jakiel, A., Palero, F., & Błażewicz, M. Deep ocean seascape and pseudotanaidae (crustacea: tanaidacea) diversity at the clarion-clipperton fracture Zone. Scientific reports, 9(1), 1-49, 2019.

Janssen, A., Kaiser, S., Meißner, K., Brenke, N., Menot, L., Arbizu, P.M.: A reverse taxonomic approach to assess macrofaunal distribution patterns in abyssal Pacific polymetallic nodule fields. PloS one 10(2), p.e0117790, 2015.

Janssen, A., Stuckas, H., Vink, A., Arbizu, P. M.: Biogeography and population structure of predominant macrofaunal taxa (Annelida and Isopoda) in abyssal polymetallic nodule fields: implications for conservation and management. Mar. Biodiv., https://doi.org/10.1007/s12526-019-00997-1, 2019.

Jennings, R. M., Brix, S., Bober, S., Svavarsson, J., Driskell, A.: More diverse than expected: distributional patterns of *Oecidiobranchus* Hessler, 1970 (Isopoda, Asellota) on the Greenland-Iceland-Faeroe Ridge based on molecular markers. Mar. Biodiv. https://doi.org/10.1007/s12526-018-0857-x, 2018.

Jennings, R. M., Etter. R. J.: Phylogeographic estimates of colonization of the deep Atlantic by the protobranch bivalve *Nucula atacellana*. Polish Polar Res 35(2): 261–278, 2014.

Jennings, R. M., Golovan, O., Brix, S.: Integrative species delimitation of desmosomatid and nannoniscid isopods from the Kuril-Kamchatka trench, with description of a hadal species. Prog. Ocean. https://doi.org/10.1016/j.pocean.2019.102236, 2020.

Johannesson, K.: "The paradox of Rockall: why is a brooding gastropod (*Littorina saxatilis*) more widespread than one having a planktonic larval dispersal stage (*L. littorea*)?." Mar. Biol. 507-513, 1988.

Kaiser, S., Barnes, D.K.A., Sands, C.J., Brandt, A.: Biodiversity of an unknown Antarctic Sea: assessing isopod richness and abundance in the first benthic survey of the Amundsen continental shelf. Mar. Biodivers. 39 (1), 27–43, 2009.

Kapli, P., Lutteropp, S., Zhang, J., Kobert, K., Pavlidis, P., Stamatakis, A., Flouri, T.: Multi-rate Poisson tree processes for single-locus species delimitation under maximum likelihood and Markov Chain Monte Carlo. Bioinformatics. 33(11), 1630-1638, 2017.

Katoh, K., Standley, D.M.: MAFFT multiple sequence alignment software version 7: improvements in performance and usability. Mol. Biol. Evol. 30(4), 772-780, 2013.

Legendre, P., Gallagher, E. D.: Ecologically meaningful transformations for ordination of species data, Oecologia 129, 271–280, https://doi.org/10.1007/s004420100716, 2001.

Kniesz, K., Brandt, A., Riehl, T.: (2017) Peritrich epibionts on the hadal isopod species *Macrostylis marionae* n. sp. from the Puerto Rico Trench used as indicator for sex-specific behaviour. DSR II Topical Studies in Oceanography DOI: 10.1016/j.dsr2.2017.10.007, 2017.

Lester, S. E., Ruttenberg, B. I., Gaines, S. D., Kinlan, B. P.: The relationship between dispersal ability and geographic range size. Ecology Letters 10(8), 745-758, 2007.

Malyutina, M. V. and Wägele, J. W. Redescription of *Storthyngura elegans* Vanhöffen, 1914 and description of a new deep-sea species of *Storthyngura* from the Peru Basin. Mitteilungen aus dem Museum für Naturkunde in Berlin, Zoologische Reihe 77(2). 2001.

Malyutina, M. V. Description of two new species of munnopsid isopods (Crustacea: Isopoda: Asellota) from manganese nodules area of the Clarion-Clipperton Fracture Zone, Pacific Ocean. Zootaxa. 2783: 1-20. 2011.

Malyutina, M. V., Frutos, I., Brandt, A.: Diversity and distribution of the deep-sea Atlantic *Acanthocope* (Crustacea, Isopoda, Munnopsidae), with description of two new species. DSR II 48, 130-150, https://doi.org/10.1016/j.dsr2.2017.11.003, 2018.

Malyutina, M., Kihara, T. C., Brix, S.: A new genus of MunnopsidaeLilljeborg, 1864 (Crustacea, Isopoda), with description of two abyssal new species from the Clarion–Clipperton Fracture, North-eastern tropical Pacific. Mar. Biodiv.

Marki, P.Z., Fjeldsa, J., Irestedt, M, Jonsson, K.A.: Molecular phylogenetics and species limits in a cryptically coloured radiation of Australo-Papuan passerine birds (Pachycephalidae: *Collurcincla*). Mol. Phylogenet. Evol. 124, 100-105, 2018.

Martínez Arbizu, P. and Haeckel, M.: RV SONNE Fahrtbericht/ Cruise Report SO239: EcoResponse Assessing the Ecology, Connectivity and Resilience of Polymetallic Nodule Field Systems, Balboa

(Panama) – Manzanillo (Mexico) 11 March–30 April 2015, GEOMAR Report, N. Ser. 025, GEOMAR Helmholtz-Zentrum für Ozeanforschung, Kiel, Germany, 2015.

McClain, C. R.., Mincks Hardy, S.: The dynamics of biogeographic ranges in the deep sea. Proc. R. Soc. B 277, 3533–3546. doi:10.1098/rspb.2010.1057, 2010.

Menzel, L., George, K. H., Arbizu, P. M.: Submarine ridges do not prevent large-scale dispersal of abyssal fauna: a case study of *Mesocletodes* (Crustacea, Copepoda, Harpacticoida). Deep Sea Research Part I: Oceanographic Research Papers 58(8), 839-864, 2011.

Miljutin, D. M., Miljutina, M. A., Arbizu, P. M., Galéron, J.: Deep-sea nematode assemblage has not recovered 26 years after experimental mining of polymetallic nodules (Clarion-Clipperton Fracture Zone, Tropical Eastern Pacific). Deep Sea Research Part I: Oceanographic Research Papers 58(8), 885-897. doi.org/10.1016/j.dsr.2011.06.003, 2011.

Oebius, H. U., Becker, H. J., Rolinski, S., Jankowskic, J. A.: Parametrization and evaluation of marine environmental impacts produced by deep-sea manganese nodule mining. DSR II: Topical Studies in Oceanography 48, 17–18, 3453-3467. doi.org/10.1016/S0967-0645(01)00052-2, 2001.

Osborn, K. J.: Relationships within the Munnopsidae (Crustacea, Isopoda, Asellota) based on three genes. Zoologica Scripta. 38, 617-635 https://doi.org/10.1111/j.1463-6409.2009.00394.x, 2009.

Osborn, K. J., Truskey, S. B., Schnurr, S., Martinez, P. M., Kaiser, S., Brenke, N., Malyutina, M., Brix, S. in prep. A test of species delimitation methods using real data with real problems.

Oksanen, J, Kindt, R., Legendre, P., O'Hara, B., Simpson, G. L., Solymos, P., Stevens, M. H. H., Wagner, H.: The vegan Package, Community ecology package 10, 631–637, 2008.

Packmoor, J. F., Mueller, F., George, K. H.: Oceanic islands and seamounts as staging posts for Copepoda Harpacticoida (Crustacea) - Shallow-water Paramesochridae Lang, 1944 from the North-East Atlantic Ocean, including the (re-)description of three species and one subspecies from the Madeiran Archipelago. Progr Oceanogr, 131:59-81, 2015.

Petersen, S., Krätschell, A., Augustin, N., Jamieson, J., Hein, J. R. Hannington, M. D.: News from the seabed – Geological characteristics and resource potential of deep-sea mineral resources. Marine Policy 70, 175-187. doi.org/10.1016/j.marpol.2016.03.012, 2016.

Pfenninger, M.., Schwenk, K.: Cryptic animal species are homogeneously distributed among taxa and biogeographical regions. BMC evolutionary biology, 7(1), 121, 2007.

Ramirez-Llodra, E., Tyler, P. A., Baker, M. C., Bergstad, O. A., Clark, M. R., Escobar, E., Lisa A. Levin, L. A., Menot, L., Rowden, A. R., Smith, C. R., Van Dover, C. L.: Man and the Last Great Wilderness: Human Impact on the Deep Sea. PLoS ONE 6(7): e22588. doi:10.1371/journal.pone.0022588, 2011.

Raupach, M. J., Malyutina, M., V., Brandt, A., Wägele, W.: Molecular data reveal a highly diverse species flock within the munnopsid deep-sea isopod *Betamorpha fusiformis* (Barnard, 1920) (Crustacea: Isopoda: Asellota) in the Southern Ocean. Deep Sea Research Part II Topical Studies in Oceanography 54(16):1820-1830. DOI: 10.1016/j.dsr2.2007.07.009, 2007.

Rex, M.: Community structure in the deep-sea benthos. Annual Review of Ecology and Systematics 12(1), 331–53. https://doi.org/10.1146/annurev.es.12.110181.001555, 1981.

Riehl, T., Brenke, N., Brix, S., Driskell, A., Kaiser, S., Brandt, A.: Field and Laboratory Methods for DNA Studies on Deep-sea Isopod Crustaceans. Polish Polar Research 35:2, 2014.

Riehl, T., Lins, L.., Brandt, A.: The effects of depth, distance, and the Mid-Atlantic Ridge on genetic differentiation of abyssal and hadal isopods (Macrostylidae). DSR II: Topical Studies in Oceanography, 148, 74-90, 2018.

Riehl, T.., Kaiser, S.: Conquered from the deep sea? A new deep-sea isopod species from the Antarctic shelf shows pattern of recent colonization. PLoS One 7 (11), e49354, 2012.

Riehl, T., De Smet, B. *Macrostylis metallicola* sp. nov.—an isopod with geographically clustered genetic variability from a polymetallic-nodule area in the Clarion-Clipperton Fracture Zone. PeerJ 8:e8621, DOI: 10.7717/peerj.8621, 2020.

Riehl, T., Golovan, O., Malyutina, M. Chapter 19. Isopoda: A review on distribution and species richness patterns along the nw Pacific. In: Saeedi H, Brandt A (2020) Biogeographic Atlas of the Deep NW Pacific Fauna. Advanced Books. https://doi.org/10.3897/ab.e51315, 2020.

Roberts, C. M., & Hawkins, J. P. Extinction risk in the sea. Trends in Ecology & Evolution, 14(6), 241-246. 1999.

Rognes, T., Flouri, T., Nichols, B., Quince, C., Mahé F. VSEARCH: a versatile open source tool for metagenomics. *PeerJ* 4:e2584. 2016.

Ronquist, F., Teslenko, M., van der Mark, P., Ayres, D.L. Darling, A., Hohna, S., Larget, B., Liu, L., Schard, M.A., Huelsenbeck, J.P. MrBayes 3.2: Efficient Bayesian phylogenetic inference and model choice across a large model space. Syst. Biol. 61(3): 539-542. 2012.

Shank T. M., Seamounts: deep-ocean laboratories of faunal connectivity, evolution, and endemism. Oceanogr 23(1), 108-122. 2010.

Sherman, C. D., Hunt, A., Ayre, D. J.: Is life history a barrier to dispersal? Contrasting patterns of genetic differentiation along an oceanographically complex coast. Biological Journal of the Linnean Society, 95(1), 106-116, 2008.

Stamatakis, A. RAxML Version 8: A tool for Phylogenetic Analysis and Post-Analysis of Large Phylogenies. Bioinformatics, 30(9), 1312-3. 2014.

Simpson, G. G.: Mammals and the nature of continents. Am. J. Sci., 241, 1–31, 1943.

Sørensen, T.: A method of establishing groups of equal amplitude in plant sociology based on similarity of species content and its application to analyses of the vegetation on Danish commons, Biol. Skr. Dan. Vid. Sel., 5, 1–34, 1948.

Suzuki, K., Yoshida, K., Watanabe, H.., Yamamoto, H.: Mapping the resilience of chemosynthetic communities in hydrothermal vent fields. Scientific ReportS 8:9364 | DOI:10.1038/s41598-018-27596-7, 2018.

Svavarsson, J.: Description of the male of *Pseudomesus brevicornis* Hansen, 1916 (Isopoda, Asellota, Desmosomatidae) and rejection of the family Pseudomesidae, Sarsia, 69:1, 37-44, DOI: 10.1080/00364827.1984.10420587, 1984.

Taboada, S., Riesgo, A., Wiklund, H., Paterson, G. L., Koutsouveli, V., Santodomingo, N., ... Glover, A. G.: Implications of population connectivity studies for the design of marine protected areas in the deep sea: An example of a demosponge from the Clarion-Clipperton Zone. Molecular ecology, 27(23), 4657-4679, 2018.

Thiel and Forschungsverbund Tiefsee-Umweltschutz (2001) Evaluation of the environmental consequences of polymetallic nodule mining based on the results of the TUSCH Research Association. Deep-Sea Research II 48, 3433-3452.

Thiel, M.., Haye, P. A.: The ecology of rafting in the marine environment. III. Biogeographical and evolutionary consequences. Oceanogr Mar Biol Annu Rev 44: 323−429, 2006.

Vanreusel, A., Hilario, A., Ribeiro, P. A., Menot, L.., Arbizu, P. M.: Threatened by mining, polymetallic nodules are required to preserve abyssal epifauna. Scientific Reports DOI: 10.1038/srep26808, 2016.

Vrijenhoek, R. C., Schutz, S. J., Gustafson, R. G. and Lutz, R. A.: Cryptic species of deep-sea clams (Mollusca: Bivalvia: Vesicomyidae) from hydrothermal vent and cold-water seep environments. Deep Sea Research Part I: Oceanographic Research Papers, 41(8), 1171-1189, 1994.

Wedding, L. M., Reiter, S. M., Smith, C. R., Gjerde, K. M., Kittinger, J. N., Friedlander, A. M., S. D. Gaines, M. R. Clark, A. M., Thurnherr, Hardy, M.., Crowder, L. B.: Managing mining of the deep seabed. Science, 349(6244), 144-145. DOI: 10.1126/science.aac6647, 2015.

Wilson, G.D.F.: Macrofauna abundance, species diversity and turnover at three sites in the Clipperton-Clarion Fracture Zone. Mar Biodiv 47: 323. https://doi.org/10.1007/s12526-016-0609-8, 2017.

Table 1. Summary of diversity parameters per sampled area. Sites = number of Epibenthic Sledge deployments, N = number of specimens, S = number of Species, Usp = number of unique species, Chao±SE = Chao estimated number of species with standard error, ACE±SE = ACE estimated number of species with standard error, H'= Shannon Diversity, 1-D= Simpson Diversity and J = Jaccard's Evenness. β_{SOR}, β_{SIM} and β_{SNE} express multiple-site total beta diversity, multiple-site species turnover and multiple-site nestedness respectively. Note that in the rows of each area the beta-diversity values are the result of excluding this area, except for the row Total (which includes all areas) and CCZ only (which includes all but APEI3 and DISCOL.

AREA	**Sites**	**N**	**S**	**Usp (%)**	**Chao±SE**	**ACE±SE**	**H'**	**1-D**	**J**	**β_{SOR}**	**β_{SIM}**	**β_{SNE}**
BGR	4	163	43	11 (25%)	49.5±4.8	53.2±3.2	3.34	0.94	0.88	0.892	0.884	0.007
IOM	3	66	40	36 (90%)	63±12.4	77±5.4	3.51	0.96	0.95	0.897	0.890	0.007
GSR	2	90	38	18 (47%)	80±25.9	69.2±5	3.34	0.95	0.91	0.900	0.894	0.005
IFREMER	2	106	50	34 (68%)	64±7.7	80.3±5.9	3.66	0.96	0.93	0.873	0.868	0.004
CCZ only	11	425	117	99 (84%)	146	137	4.21	0.97	0.80	0.767	0.746	0.021
APEI3	3	110	44	14 (32%)	59.3±9.5	63.7±4.4	3.52	0.96	0.93	0.845	0.833	0.011
DISCOL	8	84	41	31 (76%)	62.1±12.6	59.5±3.8	3.53	0.96	0.95	0.845	0.833	0.011
Total	22	619	187	-	235.46	252.15	4.76	0.98	0.91	0.885	0.878	0.007

Table 2. Faunistic similarity between areas. Number of shared species upper quadrant, number of non-shared species lower quadrant. Total number of species per site, bold in diagonal.

	43	15	16	8	1	5
	53	**40**	16	12	5	2
	49	46	**38**	11	2	4
	77	66	66	**50**	6	2
	85	74	78	82	**44**	1
	74	77	71	87	83	**41**

Table 3. Beta-diversity decomposition of Isopod Families. N = number of specimens, S = number of Species. βSOR, βSIM and βSNE express multiple-site total beta diversity, multiple-site species turnover and multiple-site nestedness respectively. Columns ccz N, ccz S, ccz βSOR, ccz βSIM and ccz βSNE consider only samples taken within the CCZ (excluding APEI3 and DISCOL).

	N	S	Chao±SE	β_{SOR}	β_{SIM}	β_{SNE}	ccz N	ccz S	ccz β_{SOR}	ccz β_{SIM}	ccz β_{SNE}
Munnopsidae	294	91	110±8.9	0.873	0.860	0.013	199	55	0.743	0.704	0.039
Desmosomatidae	143	63	98.7±17	0.904	0.895	0.009	103	43	0.817	0.802	0.014
Haploniscidae	88	24	24.6±1.1	0.916	0.898	0.0183	53	14	0.803	0.739	0.067
Macrostylidae	94	9	9.0±0.2	0.809	0.777	0.031	70	5	0.583	0.500	0.083
Total	619	187	235.46	0.885	0.878	0.007	425	117	0.767	0.746	0.021

Table 4. Number and percentage of species of the studied families present in only 1 to 6 areas. Total considers all areas together.

	1 area	**2 areas**	**3 areas**	**4 areas**	**5 areas**	**6 areas**	**Total**
Munnopsidae	69 (75.8%)	11 (12%)	7 (7.6%)	3 (3.2%)	1 (1%)	0 (0%)	91 (48.6%)
Desmosomatidae	49 (77.7%)	10 (15.8%)	3 (4.7%)	1 (1.5%)	0 (0%)	0 (0%)	63 (33.6%)
Haploniscidae	20 (83 %)	3 (12.5%)	0 (0%)	1 (4.1%)	0 (0%)	0 (0%)	24 (12.8%)
Macrostylidae	6 (66.6%)	2 (22.2%)	0 (0%)	0 (0%)	1 (11.1%)	0 (0%)	9 (4.8%)
Total	144 (77%)	26 (13.9%)	10 (5.3%)	5 (2.6%)	2 (1%)	0 (0%)	187

920

Table 5. Species distribution range by family. Data show the maximum distribution range of the species of each family excluding singletons.

Family	N	absolute max range	mean max range	mean min range
Munnopsidae	60	5245 km	800 km	253 km
Desmosomatidae	29	4480 km	628 km	40 km
Haploniscidae	19	1391 km	183 km	1 km
Macrostylidae	8	1440 km	315 km	0.13 km

925

Supplementary Table 1. Specimens used for this study including all information about station, species identification from morphology and molecular species delimitation (OTUs), museum storage and associated database numbers in BoLD and GenBank.

930 PLEASE SEE SEPARATE FILE because this is a 16 page table.

Figure 1. Map of the locations of the EBS sampling sites (red dots) within the manganese nodule contractor and the DISCOL Experimental Area (DEA) areas in the north- and south-eastern Pacific. The colourcode in this map reflects the colourcode given in the circle trees (Fig.s 2 – 5), but is not reflected

935 in the statistical graphs (Fig.s 6 – 10). In the CCZ the samples were taken in four contractor areas, from east to west: GC (dark blue - German contractor: BGR), IOM (violet - Interoceanmetal Joint Organization), BC (orange - Belgian contractor: GSR), FC (dark green - French contractor: IFREMER).

In addition, the APEI3 (red - Area of Particular Environmental Interest number 3) and DISCOL Experimental Area (light green/blue – DEA and Reference Areas).

940

Figure 2. Illustration of the locomotion of the four isopod families. From right to left: Munnopsidae – swimming, Desmosomatidae – walking/swimming, Haploniscidae – walking, Macrostylidae – burrowing.

Figure 3. Phylogenetic tree of all munnopsid samples based on 16S and COI sequences for 294 specimens. Colours indicate collection location, with black indicating outgroups. All unsupported branches were collapsed and bootstrap support indicated with asterisks indicating 100 % bootstrap support. The outer two bars summarize the results of the species delimitation analyses which included morphological determination, Vsearch for individual genes, ABGD for individual genes, PTP and mPTP for both individual genes and the concatenated datasets. The conservative bar indicates that all SD analyses supported that split, while the congruent bar indicates that the majority of SD analyses indicated that split. Numbers on congruent bars are arbitrary and provided to allow a way to refer to specific supported clades.

Figure 4. Phylogenetic tree of all desmosomatid samples based on 16S and COI sequences for 143 specimens. Colors indicate collection location, with black indicating outgroups. All unsupported branches were collapsed and bootstrap support indicated with asterisks indicating 100 % bootstrap support. The outer two bars summarize the results of the species delimitation analyses which included morphological determination, Vsearch for individual genes, ABGD for individual genes, PTP and mPTP for both individual genes and the concatenated datasets. The conservative bar indicates that all SD analyses supported that split, while the congruent bar indicates that the majority of SD analyses indicated that split. Numbers on congruent bars are arbitrary and provided to allow a way to refer to specific supported clades.

Figure 5. Phylogenetic tree of all haploniscid samples based on 16S and COI sequences for 88 specimens. Colors indicate collection location, with black indicating outgroups. All unsupported branches were collapsed and bootstrap support indicated with asterisks indicating 100 % bootstrap support. The outer two bars summarize the results of the species delimitation analyses which included morphological determination, Vsearch for individual genes, ABGD for individual genes, PTP and mPTP for both individual genes and the concatenated datasets. The conservative bar indicates that all SD analyses supported that split, while the congruent bar indicates that the majority of SD analyses indicated that split. Numbers on congruent bars are arbitrary and provided to allow a way to refer to specific supported clades.

Figure 6. Phylogenetic tree of all macrostylid samples based on 16S and COI sequences for 94 specimens. Colors indicate collection location, with black indicating outgroups. All unsupported branches were collapsed and bootstrap support indicated with asterisks indicating 100 % bootstrap support. The outer two bars summarize the results of the species delimitation analyses which included morphological determination, Vsearch for individual genes, ABGD for individual genes, PTP and mPTP for both individual genes and the concatenated datasets. The conservative bar indicates that all SD analyses supported that split, while the congruent bar indicates that the majority of SD analyses indicated that split. Numbers on congruent bars are arbitrary and provided to allow a way to refer to specific supported clades.

Figure 7. Rarefaction analysis by isopod family, considering all areas together.

Figure 8. Rarefaction analysis by area, considering all families together.

945 **Figure 9.** nMDS ordination plot of Chord-distance between areas.

Figure 10. nMDS ordination plot of Euclidean-distance between areas of presence-absence transformed data.

Figure 11. Box and whiskers plot showing the median and range of the Chord distance of every area to other areas.

Figure 12. Upset plot showing the number of species shared between sampling sites. The lower panel shows the sets of combination of sites. Sites sharing species are indicated by dots joined by a vertical line. The corresponding bar in the upper panel shows the number species co-occurring in this particular set of stations.

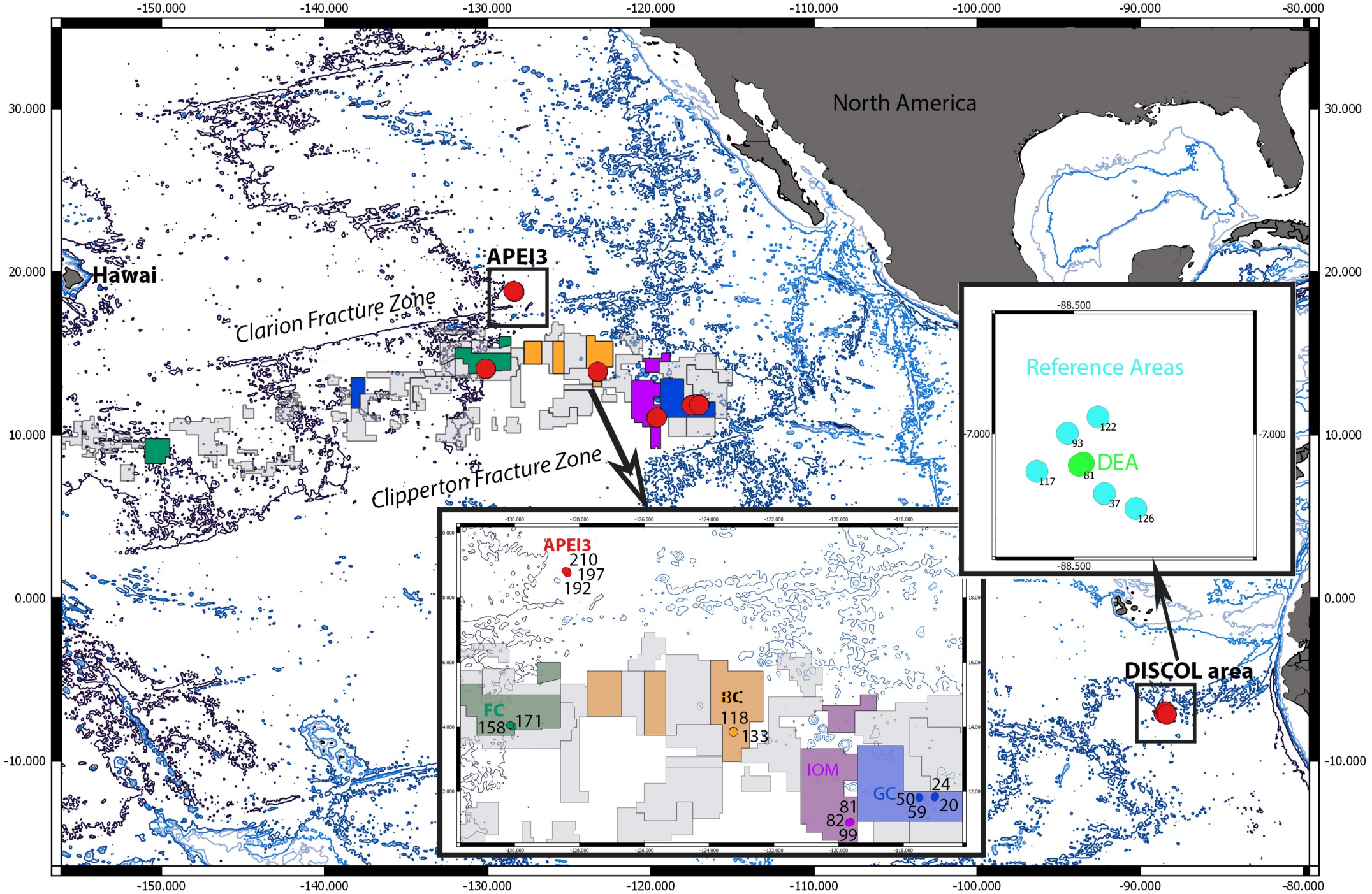
North America
Hawai
APEI3
Clarion Fracture Zone
Clipperton Fracture Zone
DISCOL area
Reference Areas
DEA
122
93
81
117
37
126
-88.500
-7.000
APEI3
210
197
192
FC
158
171
BC
118
133
IOM
GC
24
50
59
20
81
82
99
-150.000
-140.000
-130.000
-120.000
-110.000
-100.000
-90.000
-80.000
30.000
20.000
10.000
0.000
-10.000

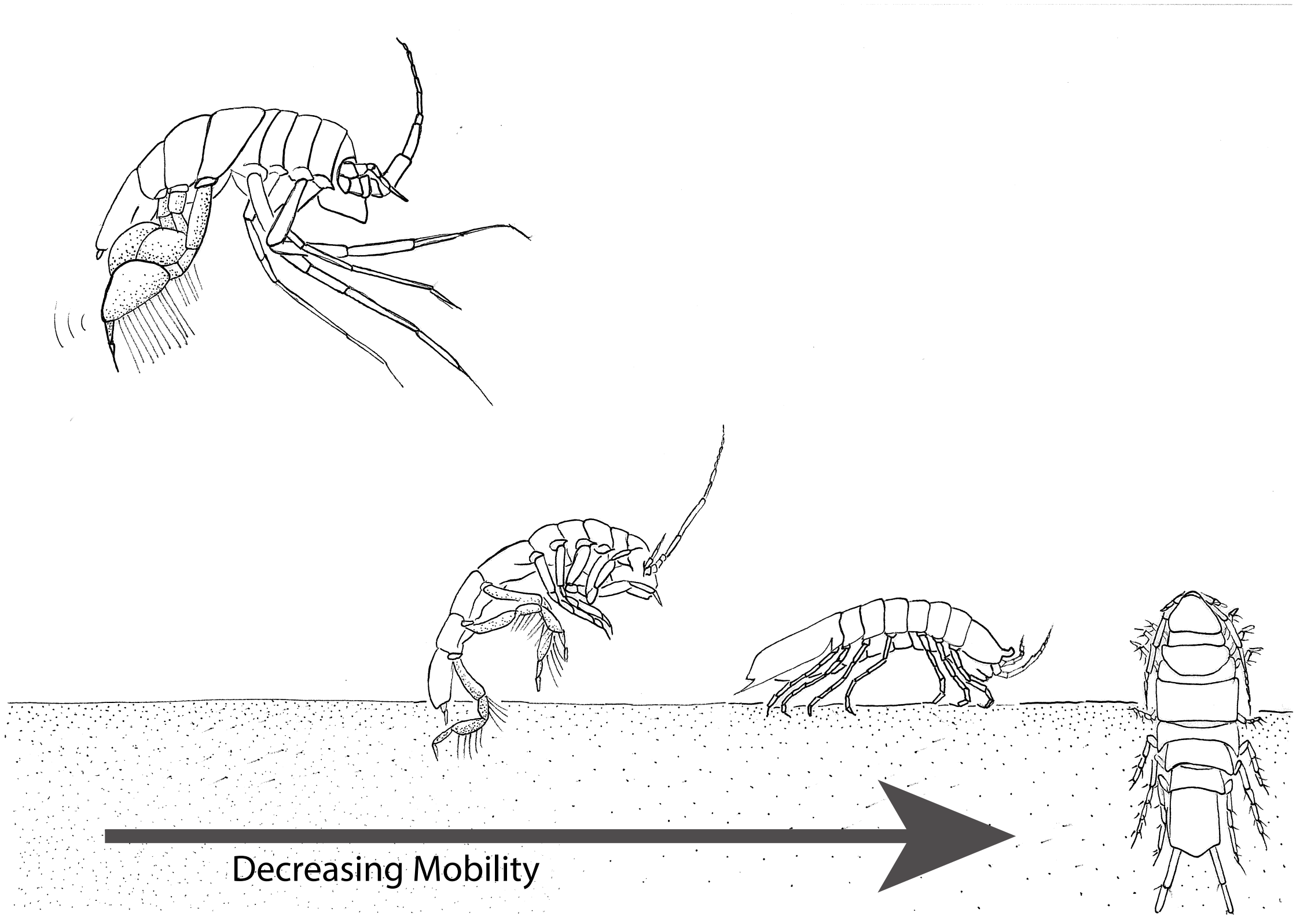
Decreasing Mobility

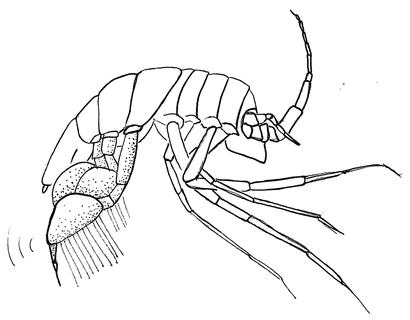

APEI3
BGR
IOM
GSR
IFREMER
DISCOL

0.4

Conserv.
Congruent

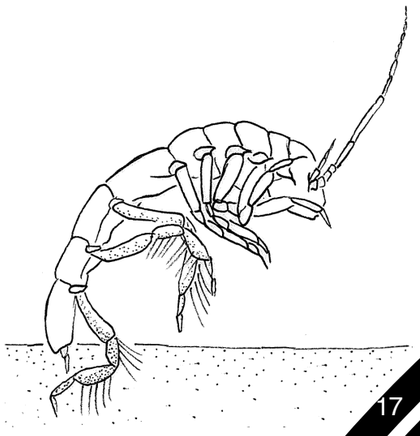

APEI3
BGR
IOM
GSR
IFREMER
DISCOL

DesmJP064_*Chelator_DisparellaUncertain*_IOM
DesmJP077_*PDisparella*_BC
DesmJP103_*Disparella*__FC
DesmJP075_cf_*Disparella*__BC
DesmJP148_cf_*Disparella*__A3
DesmJP140_*Chelator_DisparellaUncertain*_A3
DesmJP143_cf_*Disparella*__A3
DesmJP093_cf Disparella_sp1_BC
DesmJP021_*Disparella*_sp1_GC
DesmJP012_*Disparella*_sp1_GC
DesmJP013_cf_*Disparella*_sp1_GC
DesmDi30_Disparella_sp01_RHN
DesmJP125_*Disparella*__A3
DesmJP054_*Mirabilicoxa*_spC_IOM
DesmJP027_*Mirabilicoxa*_sp1_GC
DesmJP004_*Mirabilicoxa*_sp1_GC
DesmJP006_*Mirabilicoxa*_sp1_GC
DesmJP017_*Mirabilicoxa*_sp1_GC
DesmJP041_*Mirabilicoxa*_sp1_GC
DesmDi23_*Mirabilicoxa*_sp3_DEA
DesmDi08_*Mirabilicoxa*_sp3_RHN
DesmDi07_*Mirabilicoxa*_sp3_RS
DesmJP116_cf_*Mirabilicoxa*_spA_FC
DesmJP115_cf_*Mirabilicoxa*_spA_FC
DesmJP105_*Mirabilicoxa*_spA_FC
DesmJP111_*Mirabilicoxa*_spA_FC
DesmJP118_*Mirabilicoxa*_spA_FC
DesmJP073_*Mirabilicoxa*_spA_IOM
DesmJP121_*Prochelator*__FC
DesmJP082_*Prochelator*__BC
DesmDi11_*Prochelator*_sp01_RNw
DesmJP028_*Prochelator*_GC
DesmJP049_*Prochelator*_GC
DesmJP085_*Prochelator*_BC
DesmJP096_*Prochelator*_BC
DesmJP040_*Prochelator*_GC
DesmJP010_*Prochelator*_GC
DesmJP127_*Prochelator*_FC
DesmJP113_*Prochelator*_BC
DesmJP078_cf_*Prochelator*_BC
DesmJP086_*Prochelator*_BC
DesmJP087_*Prochelator*_BC
DesmJP088_*Prochelator*_BC
DesmJP123_*Prochelator*_FC
DesmDi28_Eugerdella_sp12_RHN
DesmJP126_*Eugerdella*_sp6Uncertain_A3
DesmJP147_*Eugerdella*_sp6Uncertain_A3
DesmJP162_*Eugerdella*_sp6Uncertain_A3
DesmJP051_cf_*Prochelator*_IOM
DesmJP068_*Eugerdella*_sp6_IOM
DesmJP057_*Eugerdella*_5or6_IOM
DesmJP065_*Eugerdella*_sp5_IOM
DesmJP055_cf_*Eugerdella*_IOM
DesmJP104_*Mirabilicoxa*_FC
DesmJP109_*Eugerdella*_sp6_FC
DesmJP142_*Eugerdella*_sp6Uncertain_A3
DesmJP042_*Eugerdella*_sp10_GC
DesmJP046_*Eugerdella*_sp10_GC
DesmJP043_*Eugerdella*_sp10_GC
DesmJP081_*Eugerdella*_sp10_BC
DesmJP008_Eugerdella_GC
DesmJP001_Eugerdella_sp11_GC
DesmJP019_Eugerdella_sp11_GC
DesmJP069_Eugerdella_sp11_IOM
DesmJP023_Eugerdella_sp11_GC
DesmJP059_Eugerdella_sp11_IOM
DesmJP039_Eugerdella_s11_GC
DesmJP016_Eugerdella_sp11_GC
DesmJP009_Eugerdella__GC
DesmJP024_Eugerdella_sp11_GC
DesmJP101_Eugerdella_sp8_FC
DesmJP007_Eugerdella_sp9_GC
DesmJP005_Eugerdella_sp9_GC
DesmJP071_Eugerdella_sp3_IOM
DesmJP076_Eugerdella_spcf7_BC
DesmJP110_Eugerdella_sp7_FC
DesmJP084_Eugerdella_sp5_BC
DesmJP053_Eugerdella_sp5_IOM
DesmJP117_Eugerdella_sp5_FC
DesmJP094_Eugerdella_sp5_BC
DesmJP120_Eugerdella_sp5_FC
DesmJP095_Eugerdella_sp5_BC
DesmJP112_Eugerdella_sp5_FC
DesmJP022_cf_Eugerdella_sp2_GC
DesmJP074_Eugerdella_cfegoni_BC
DesmJP092_Eugerdella_cfegoni_GC
DesmJP031_Eugerdella_BC
DesmJP037_Eugerdella_sp01_RHN
DesmDi31_Eugerda_sp01_DEA
DesmDi09_Eugerda_sp01_RS
DesmDi03 Eugerdella/Eugerda indet RS
DesmDi02 Eu / Des? sp03 RS
EF682292_*Betamorpha_africana*_G6
Ef116524_*Betamorpha_fusiformis*_BF7
Ef116525_*Betamorpha_fusiformis*_BF9
Ef116528_*Betamorpha_fusiformis*_BF12
Ef116527_*Betamorpha_fusiformis*_BF11
DesmJP138_*Chelator*_spA_A3
DesmJP139_*Chelator*_spA_A3
DesmJP145_cf_*Chelator*_spA_A3
DesmJP133_*Chelator*_spA_A3
DesmDi12_*Chelator*_sp01_RNw
DesmJP119_*Chelator*_spB_FC
DesmJP159_cf_*Chelator*_spC_A3
DesmJP153_*Chelator*_spC_A3
DesmJP152_*Chelator*_spC_A3
DesmJP091_*Chelator*_spD_BC
DesmDi20_*Chelator*_sp02_Rwo
DesmJP061_*Chelator*_spD_IOM
DesmJP050_*Chelator*_spD_IOM
DesmJP060_*Chelator*_spD_IOM
DesmJP135_cf_*Oecidiobranchus*_*oeci*_A3
DesmJP154_cf_*Oecidiobranchus*_*oeci*_A3
DesmJP137_cf_*Oecidiobranchus*_*oeci*_A3
DesmJP020_*Mirabilicoxa*_spC_GC
DesmJP038_*Mirabilicoxa*_spC_GC
DesmJP048_cf_*Mirabilicoxa*_spC_GC
DesmJP002_*Mirabilicoxa*_spC_GC
DesmJP134_cf_*Mirabilicoxa*_spB_A3
DesmJP131_*Mirabilicoxa*_spB_A3
DesmJP107_cf_*Mirabilicoxa*_spB_FC
DesmJP128_cf_*Mirabilicoxa*_spB_A3
DesmJP099_*Mirabilicoxa*_spD_FC
DesmJP083_*Mirabilicoxa*_spD_BC
DesmJP011_*Mirabilicoxa*_spD_GC
DesmJP066_*Mirabilicoxa*_spD_IOM
DesmJP033_*Mirabilicoxa*_spD_GC
DesmJP108_cf_*Mirabilicoxa*_spE_FC
DesmJP114_cf_*Mirabilicoxa*_spE_FC
DesmJP106_*Mirabilicoxa*_spE_FC
DesmJP100_*Mirabilicoxa*_spE_FC
DesmJP015_*Mirabilicoxa*_spF_GC
DesmJP025_*Mirabilicoxa*_spF_GC
DesmJP032_*Mirabilicoxa*_spF_GC
DesmJP067_*Mirabilicoxa*_IOM
DesmJP018_cf_*Mirabilicoxa*_GC
DesmDi24_*Mirabilicoxa*_sp01_Rwo
DesmDi21_*Mirabilicoxa*_sp01_RNw
DesmJP160_*Mirabilicoxa*_indet_A3
DesmJP129_*Mirabilicoxa*_A3
DesmJP124_*Mirabilicoxa*_A3
DesmJP045_*Eugerdella*_sp3_GC
DesmJP030_*Eugerdella*_sp4_GC
DesmJP026_*Eugerdella*_sp3_GC
DesmDi17_*Eugerdella*_sp01_RNw
DesmJP034_*Eugerdella*_sp3_GC
DesmJP047_*Eugerdella*_sp3_GC

0.3

Conservative
Congruent

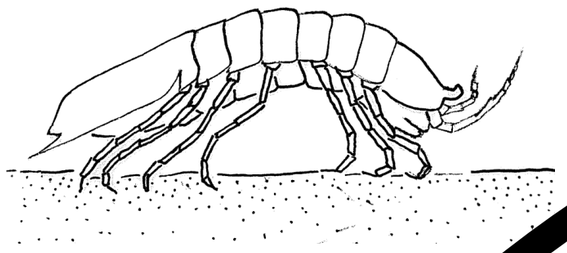

APEI3
BGR
IOM
GSR
IFREMER
DISCOL

HaplJP071_*Haploniscus*_sp2_A3
HaplJP062_*Haploniscus*_sp2_A3
HaplJP065_*Haploniscus*_sp2_A3
HaplJP060_*Haploniscus*_sp2_A3
HaplJP058_*Haploniscus*_sp2_A3
HaplJP067_*Haploniscus*_sp2_A3
HaplJP070_*Haploniscus*_sp2_FC
HaplJP054_*Haploniscus*_sp2_FC
HaplJP049_*Haploniscus*_sp2_FC
HaplJP050_*Haploniscus*_sp2_FC
HaplJP043_*Haploniscus*_sp2_FC
HaplJP019_*Haploniscus*_sp2_IOM
HaplJP032_*Haploniscus*_sp2_BC
HaplJP033_*Haploniscus*_sp2_BC
HaplJP016_*Haploniscus*_sp2_GC
HaplJP013_*Haploniscus*_sp2_GC
HaplJP015_*Haploniscus*_sp2_GC
HaplJP010_*Haploniscus*_sp2_GC
HaplJP014_*Haploniscus*_sp2_GC
HaplJP022_*Haploniscus*_sp2_IOM
HaplDi24_*Chauliodoniscus*_sp01_RNw
HaplJP003_*Haploniscus*_sp2_GC
HaplJP006_*Haploniscus*_sp2_GC
HaplJP061_*Mastigoniscus*_sp5_A3
HaplJP059_*Haploniscus*_sp5_A3
HaplJP020_*Haploniscus*_sp5_IOM
HaplJP064_*Mastigoniscus*_sp5_A3
HaplDi05_cf_*Chauliodoniscus*_nov._sp._01_RNw
HaplDi19_cf_*Chauliodoniscus*_DEA
HaplDi16_cf_*Chauliodoniscus*_nov._sp._01_RNw
HaplDi12_cf_*Chauliodoniscus*_nov._sp._01_RNw
HaplDi14_cf_*Chauliodoniscus*_nov._sp._01_RNw
HaplJP008_*Haploniscus*_sp4_GC
HaplJP045_*Haploniscus*_sp1_FC
HaplJP046_*Haploniscus*_sp1_FC
HaplJP044_*Haploniscus*_sp1a_FC
HaplJP052_*Haploniscus*_sp1_FC
HaplJP055_*Haploniscus*_sp1_FC
HaplJP057_*Mastigoniscus*_sp8_A3
HaplJP072_*Mastigoniscus*_sp8_A3
HaplJP063_*Mastigoniscus*_sp3_A3
HaplJP066_*Mastigoniscus*_sp3_A3
*laniropsis_epilittoralis*_2
*laniropsis_epilittoralis*_1
HaplJP074_*Mastigoniscus*_sp3_IOM
HaplJP021_*Mastigoniscus*_sp3_IOM
HaplJP031_*Mastigoniscus*_sp3_BC
HaplJP023_*Mastigoniscus*_sp3_BC
HaplJP040_*Mastigoniscus*_sp3_BC
HaplJP036_*Mastigoniscus*_sp_BC
HaplJP034_*Mastigoniscus*_sp3_BC
HaplJP028_*Mastigoniscus*_sp3_BC
HaplJP035_*Mastigoniscus*_sp3_BC
HaplJP037_*Mastigoniscus*_sp3_BC
HaplJP025_*Mastigoniscus*_sp3_BC
HaplJP026_*Mastigoniscus*_sp3_BC
HaplDi15_*Chauliodoniscus*_sp01_RNw
HaplDi09_*Chauliodoniscus*_sp01_RNw
HaplJP041_*Mastigoniscus*_sp_nov3_BIONOD_FC
HaplJP048_*Mastigoniscus*_sp3_FC
HaplJP051_*Mastigoniscus*_sp3_FC
HaplJP068_*Mastigoniscus*_sp5_A3
HaplJP069_*Mastigoniscus*_sp5_A3
HaplJP073_*Haploniscus*_sp5_A3
HaplJP024_*Mastigoniscus*_sp3007_BC
HaplJP029_*Mastigoniscus*_sp3007_BC
HaplJP038_*Mastigoniscus*_sp3007_BC
HaplJP027_*Mastigoniscus*_sp3007_BC
HaplJP039_*Mastigoniscus*_sp3007_BC
HaplJP042_*Mastigoniscus*_sp3007_FC
HaplJP002_*Mastigoniscus*_sp3Brokeland_GC
HaplJP004_*Mastigoniscus*_sp3Brokeland_GC
HaplJP009_*Mastigoniscus*_sp3Brokeland_GC
HaplJP005_*Mastigoniscus*_sp3Brokeland_GC
HaplJP001_*Mastigoniscus*_sp5_GC
HaplJP011_*Mastigoniscus*_sp5_IOM
HaplJP018_*Mastigoniscus*_sp5_GC
HaplJP017_*Mastigoniscus*_sp5_GC
HaplDi13_*Chauliodoniscus*_sp01_RNw
HaplDi02_*Chauliodobiscus*_sp01_RNw
HaplDi03_*Chauliodobiscus*_sp01_RNw
HaplDi04_*Chauliodoniscus*_sp01_RNw
HaplDi11_*Chauliodoniscus*_sp01_RNw
HaplDi17_*Chauliodoniscus*_sp01_RNw
HaplDi07_*Chauliodoniscus*_sp01_RNw
HaplDi08_*Chauliodoniscus*_sp01_RNw
HaplDi18_*Chauliodoniscus*_sp01_RNw
HaplJP053_*Haploniscus*_sp7_FC
HaplJP047_*Haploniscus*_sp7_FC

0.2

Conservative
Congruent

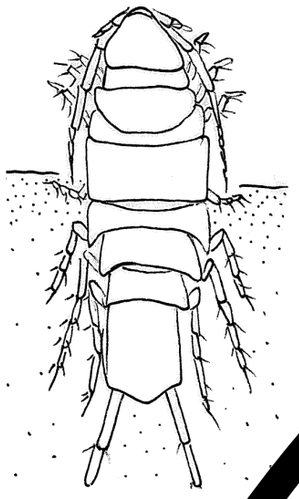

APEI3
BGR
IOM
GSR
IFREMER
DISCOL

MacrJP063_Macrostylis_spM_FC
MacrJP070_Macrostylis_spM_FC
MacrJP068_Macrostylis_spM_FC
MacrJP059_Macrostylis_spM_FC
MacrJP064_Macrostylis_spM_FC
MacrJP058_Macrostylis_spM_FC
MacrJP066_Macrostylis_spM_FC
MacrJP065_Macrostylis_spM_FC
MacrJP071_Macrostylis_spM_FC
MacrJP073_Macrostylis_spM_A3
MacrJP069_Macrostylis_spM_FC
MacrJP036_Macrostylis_spM_IOM
MacrJP041_Macrostylis_spM_IOM
MacrJP042_Macrostylis_spM_IOM
MacrJP039_Macrostylis_spM_IOM
MacrJP040_Macrostylis_spM_IOM
MacrJP052_Macrostylis_spM_BC
MacrJP044_Macrostylis_spM_BC
MacrJP048_Macrostylis_spM_BC
MacrJP049_Macrostylis_spM_BC
MacrJP043_Macrostylis_spM_BC
MacrJP045_Macrostylis_spM_BC
MacrJP026_Macrostylis_spM_GC
MacrJP030_Macrostylis_spM_GC
MacrJP031_Macrostylis_spM_GC
MacrJP028_Macrostylis_spM_GC
MacrJP034_Macrostylis_spM_GC
MacrJP032_Macrostylis_spM_GC
MacrJP027_Macrostylis_spM_GC
MacrJP033_Macrostylis_spM_GC
MacrJP046_Macrostylis_spM_BC
MacrJP047_Macrostylis_spM_BC
MacrJP083_Macrostylis_sp2_A3
MacrJP091_Macrostylis_sp2_A3
MacrJP074_Macrostylis_sp2_A3
MacrJP087_Macrostylis_sp2_A3
MacrJP085_Macrostylis_sp2_A3
MacrJP088_Macrostylis_sp3_A3
MacrJP086_Macrostylis_sp2_A3
MacrJP084_Macrostylis_sp2_A3
MacrJP005_Macrostylis_sp1_GC
MacrJP017_Macrostylis_sp1_GC
MacrJP016_Macrostylis_cfsp1_GC
MacrJP010_Macrostylis_spM_GC
MacrJP038_Macrostylis_cfsp1_IOM
KY951731_Thaumastosoma_diva_D3D64
Thaumastosoma_platycarpus_IDesm10
KM14_Iso261_Ketosoma_sp._2
KY951729_Ketosoma_hessleri_VT569
Ketosoma_vemae_VTDes013
MacrDi09_Macrostylis_sp03_FNw
MacrDi08_Macrostylis_sp03_DEA
MacrDi04_Macrostylis_sp03_RS
MacrDi07_Macrostylis_sp03_DEA
MacrJP062_Macrostylis_spM_FC
MacrJP050_Macrostylis_spM_BC
MacrJP054_Macrostylis_spM_BC
MacrJP053_Macrostylis_spM_BC
MacrJP055_Macrostylis_spM_FC
MacrJP061_Macrostylis_spM_FC
MacrJP067_Macrostylis_spM_FC
MacrJP060_Macrostylis_spM_FC
MacrJP057_Macrostylis_spM_FC
MacrJP072_Macrostylis_spM_FC
MacrJP090_Macrostylis_spM_A3
MacrJP078_Macrostylis_spM_A3
MacrJP077_Macrostylis_spM_A3
MacrJP080_Macrostylis_spM_A3
MacrJP079_Macrostylis_spM_A3
MacrJP082_Macrostylis_spM_A3
MacrJP081_Macrostylis_spM_A3
MacrJP089_Macrostylis_spM_A3
MacrJP075_Macrostylis_spM_A3
MacrJP076_Macrostylis_spM_A3
MacrJP023_Macrostylis_spM_GC
MacrJP014_Macrostylis_spM_GC
MacrJP035_Macrostylis_spM_IOM
MacrJP037_Macrostylis_spM_IOM
MacrJP022_Macrostylis_spM_GC
MacrJP021_Macrostylis_spM_GC
MacrJP025_Macrostylis_spM_GC
MacrJP024_Macrostylis_spM_GC
MacrJP029_Macrostylis_spM_GC
MacrJP013_Macrostylis_spM_GC
MacrJP020_Macrostylis_spM_GC
MacrJP009_Macrostylis_spM_GC
MacrJP019_Macrostylis_spM_GC
MacrJP015_Macrostylis_spM_GC
MacrJP011_Macrostylis_spM_GC
MacrJP001_Macrostylis_spM_GC
MacrJP002_Macrostylis_spM_GC
MacrJP018_Macrostylis_spM_GC
MacrJP003_Macrostylis_spM_GC
MacrJP007_Macrostylis_spM_GC
MacrJP012_Macrostylis_spM_GC
MacrJP004_Macrostylis_spM_GC
MacrJP006_Macrostylis_spM_GC
MacrJP008_Macrostylis_spM_GC

0.2

Conservative
Congruent

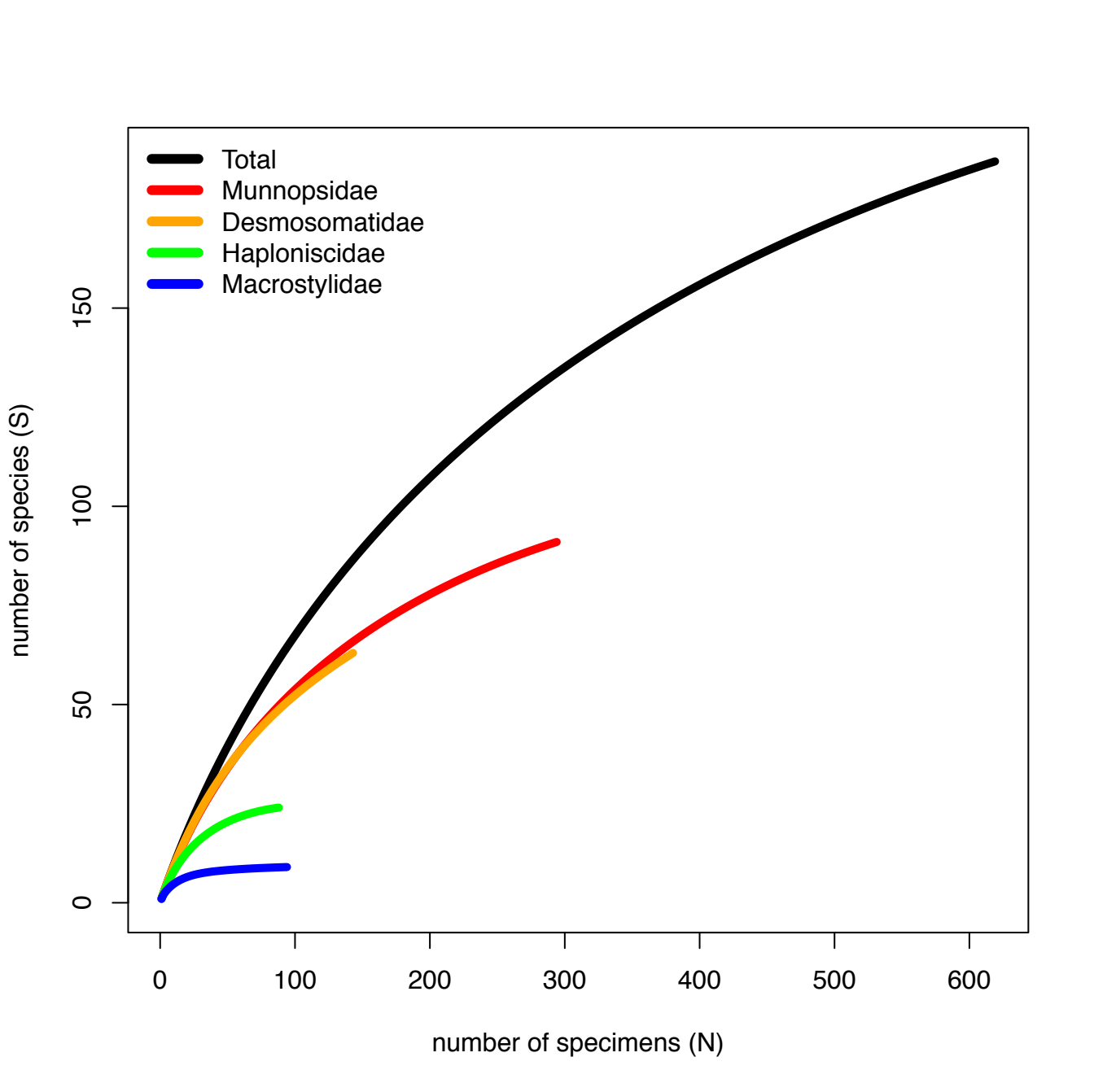
Total
Munnopsidae
Desmosomatidae
Haploniscidae
Macrostylidae
number of species (S)
0
50
100
150
0
100
200
300
400
500
600
number of specimens (N)

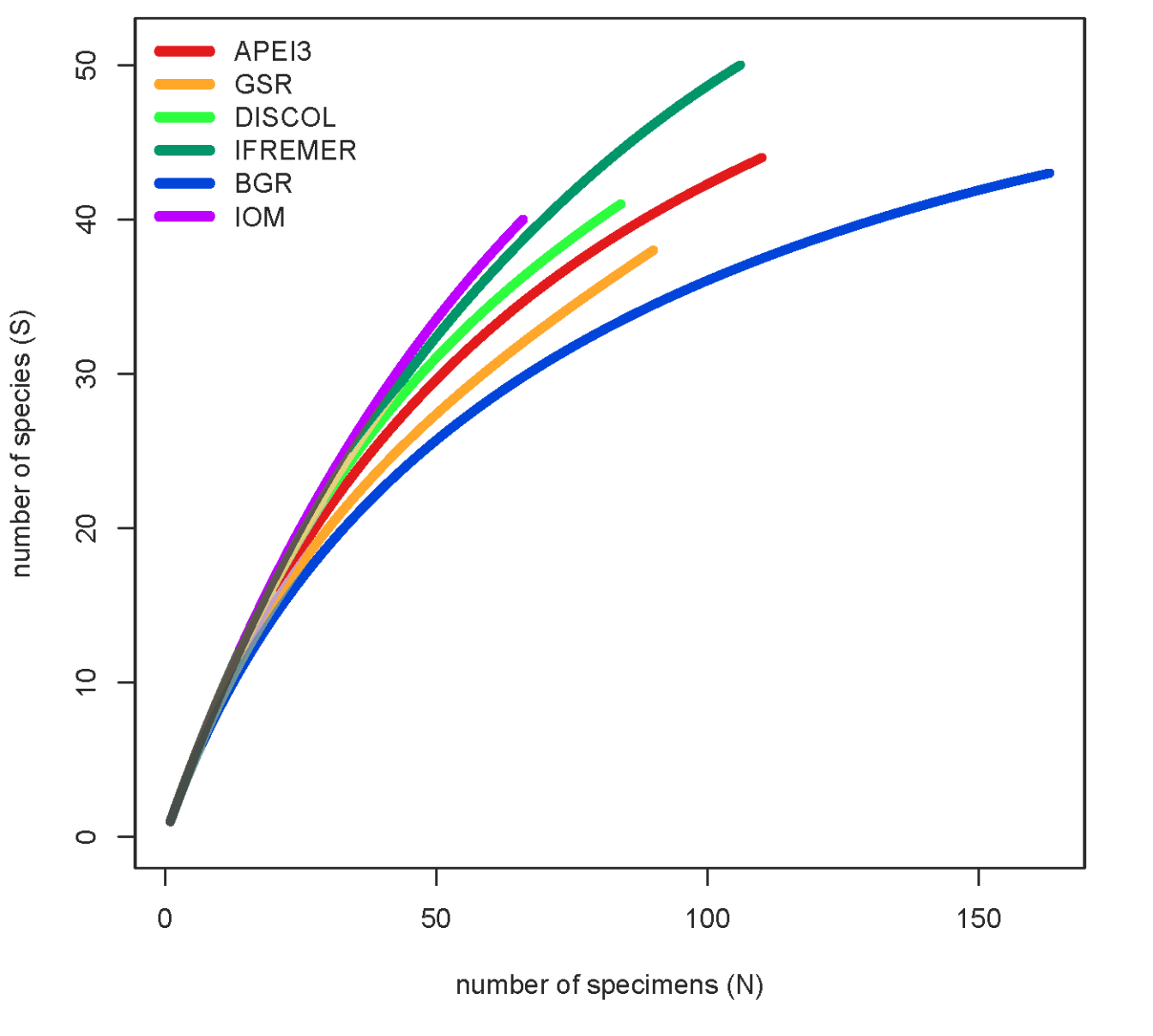
APEI3
GSR
DISCOL
IFREMER
BGR
IOM
number of species (S)
0
10
20
30
40
50
0
50
100
150
number of specimens (N)

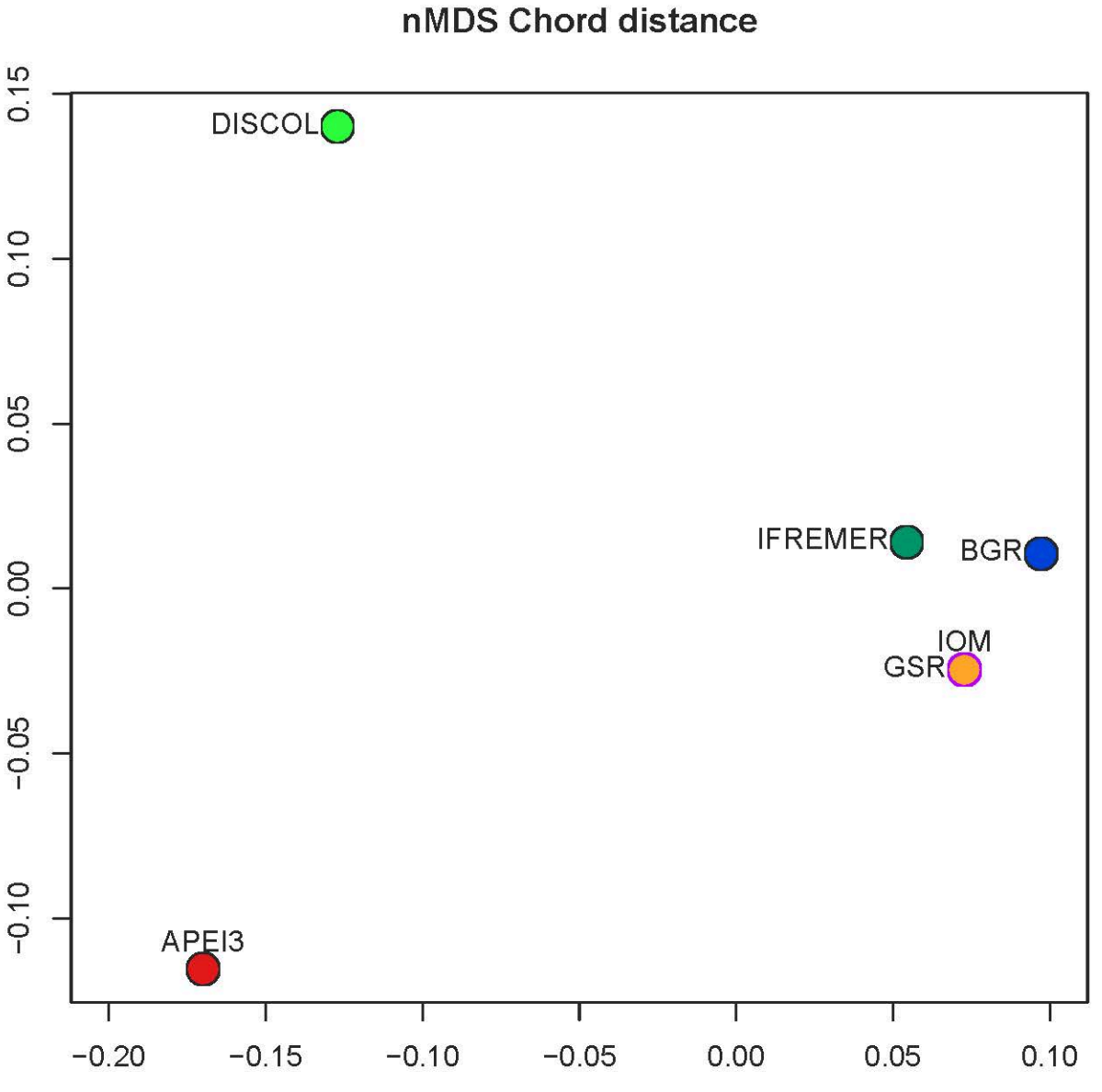
nMDS Chord distance
DISCOL
IFREMER
BGR
IOM
GSR
APEI3
0.15
0.10
0.05
0.00
−0.05
−0.10
−0.20
−0.15
−0.10
−0.05
0.00
0.05
0.10

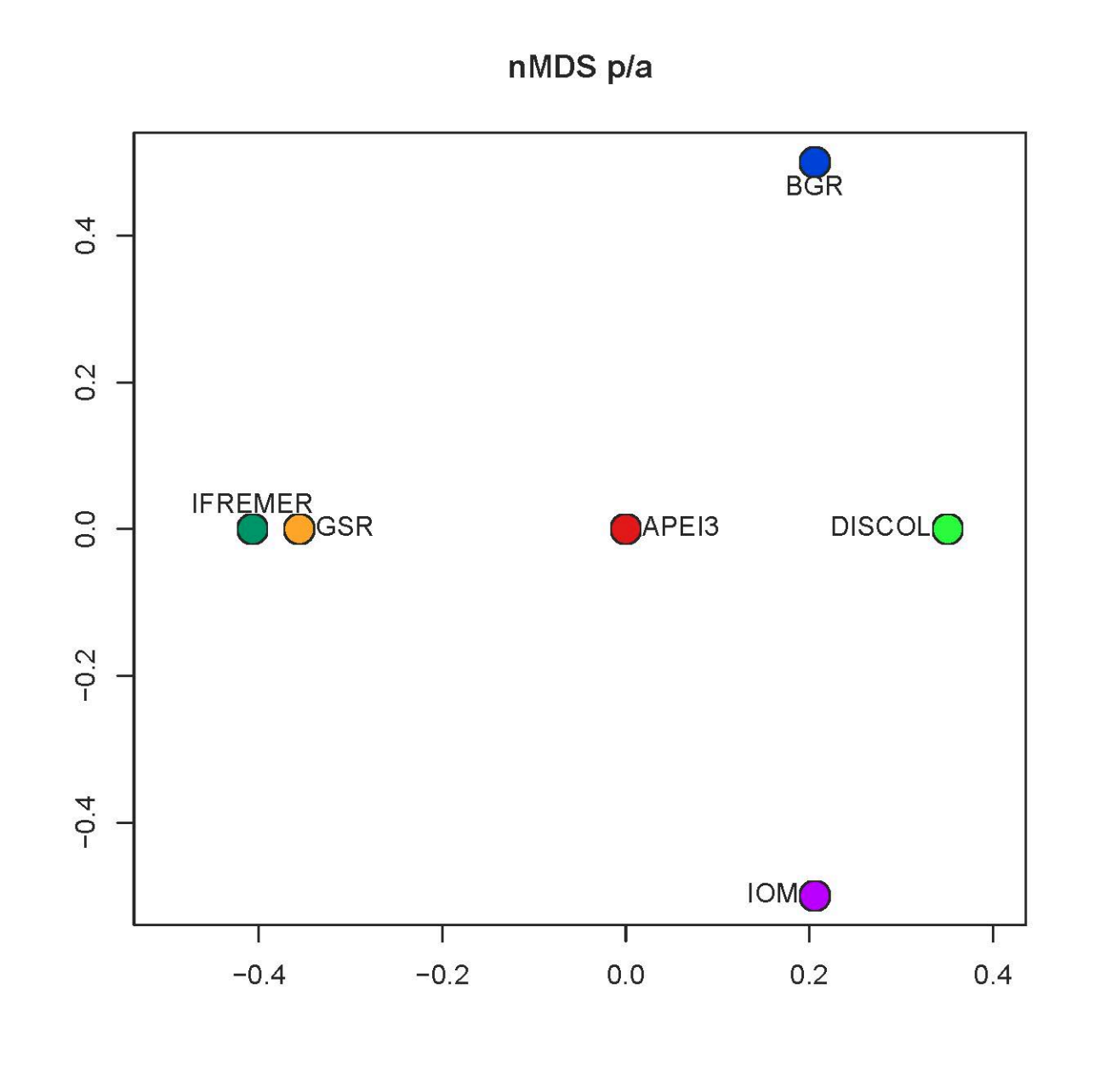
nMDS p/a
BGR
IFREMER
GSR
APEI3
DISCOL
IOM
0.4
0.2
0.0
−0.2
−0.4
−0.4
−0.2
0.0
0.2
0.4

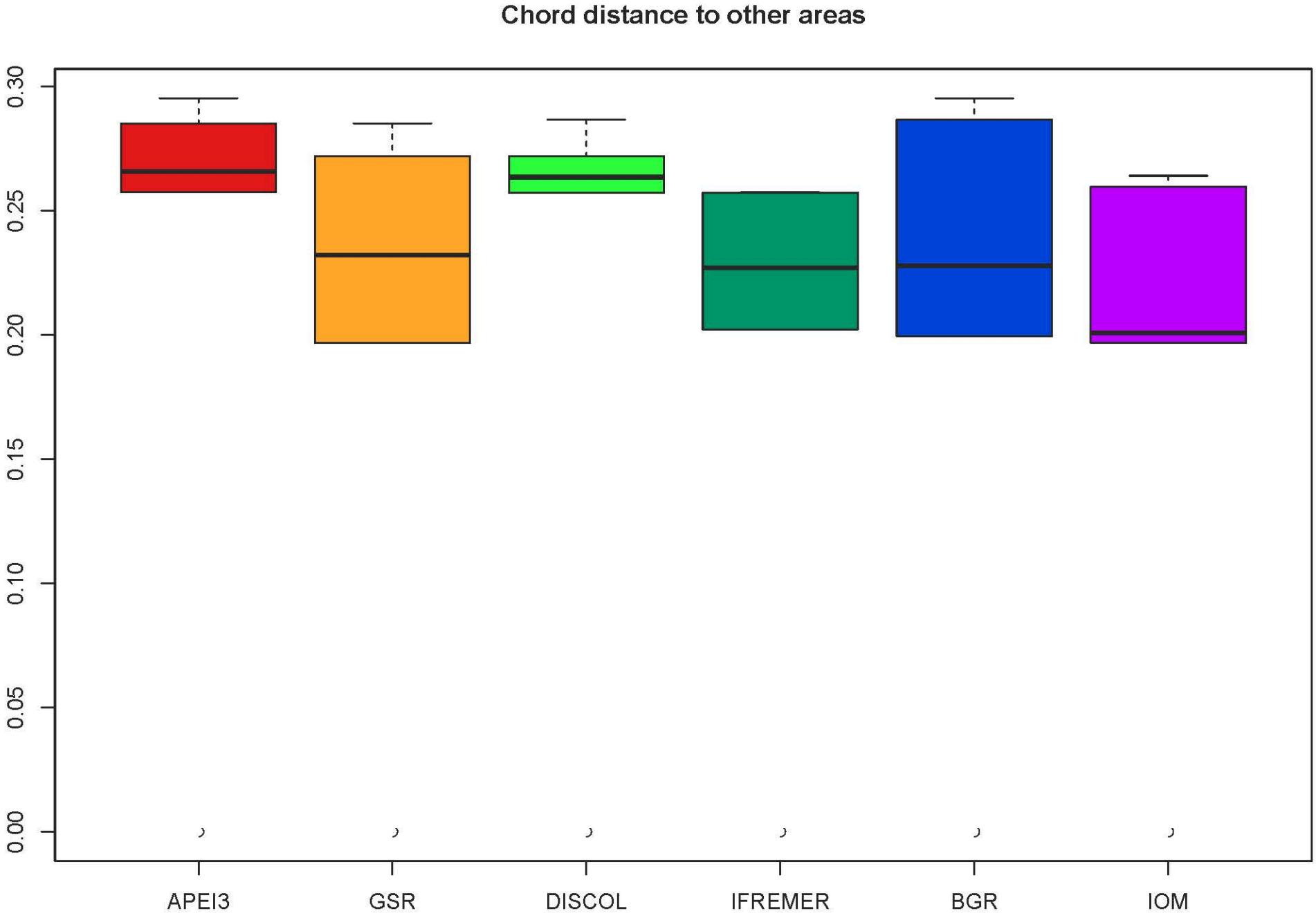
Chord distance to other areas
0.00
0.05
0.10
0.15
0.20
0.25
0.30
APEI3
GSR
DISCOL
IFREMER
BGR
IOM

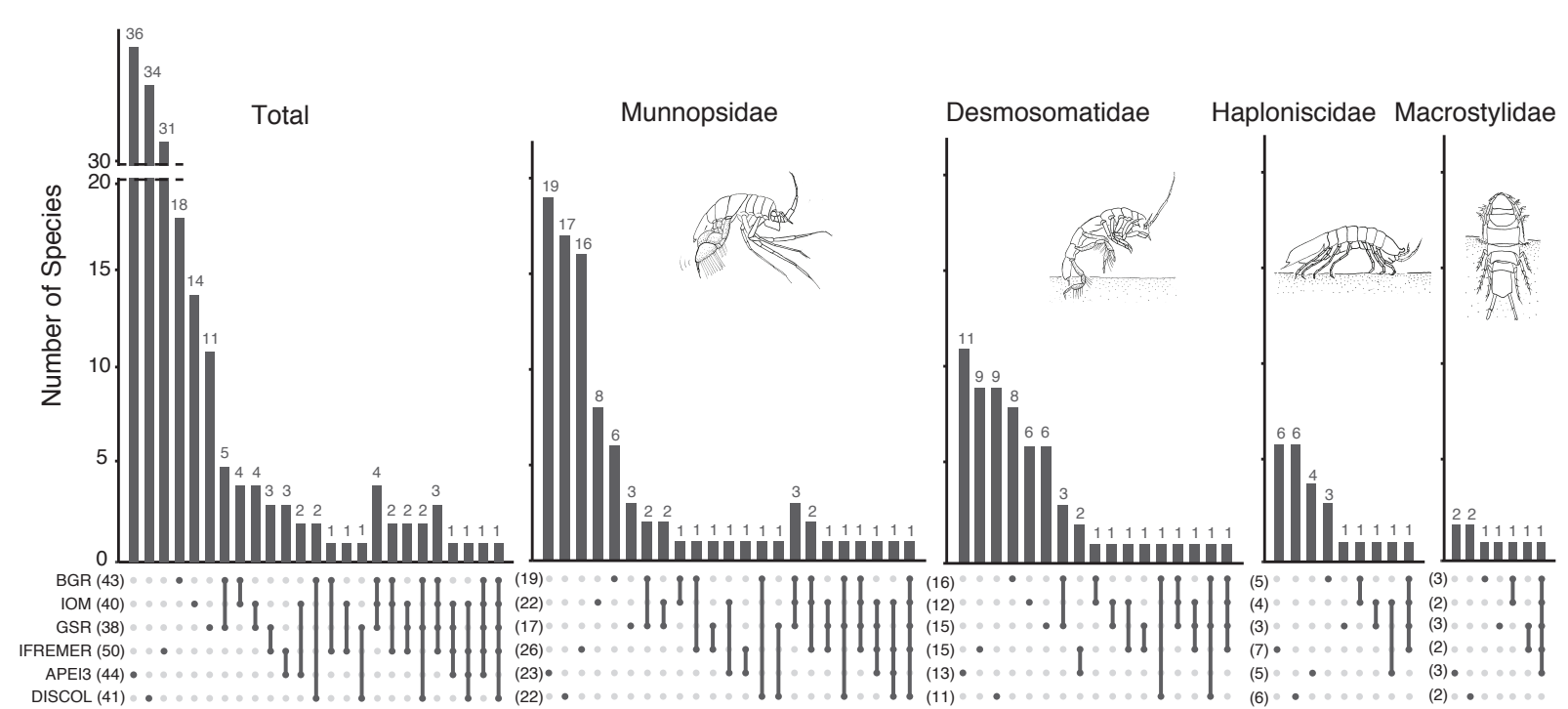
Number of Species
0
5
10
15
20
30
Total
36
34
31
18
14
11
5
4
4
3
3
2
2
1
1
1
4
2
2
2
3
1
1
1
1
Munnopsidae
19
17
16
8
6
3
2
2
1
1
1
1
1
1
1
3
2
1
1
1
1
1
1
Desmosomatidae
11
9
9
8
6
6
3
2
1
1
1
1
1
1
1
1
1
Haploniscidae
6
6
4
3
1
1
1
1
1
Macrostylidae
2
2
1
1
1
1
1
BGR (43)
IOM (40)
GSR (38)
IFREMER (50)
APEI3 (44)
DISCOL (41)
(19)
(22)
(17)
(26)
(23)
(22)
(16)
(12)
(15)
(15)
(13)
(11)
(5)
(4)
(3)
(7)
(5)
(6)
(3)
(2)
(3)
(2)
(3)
(2)

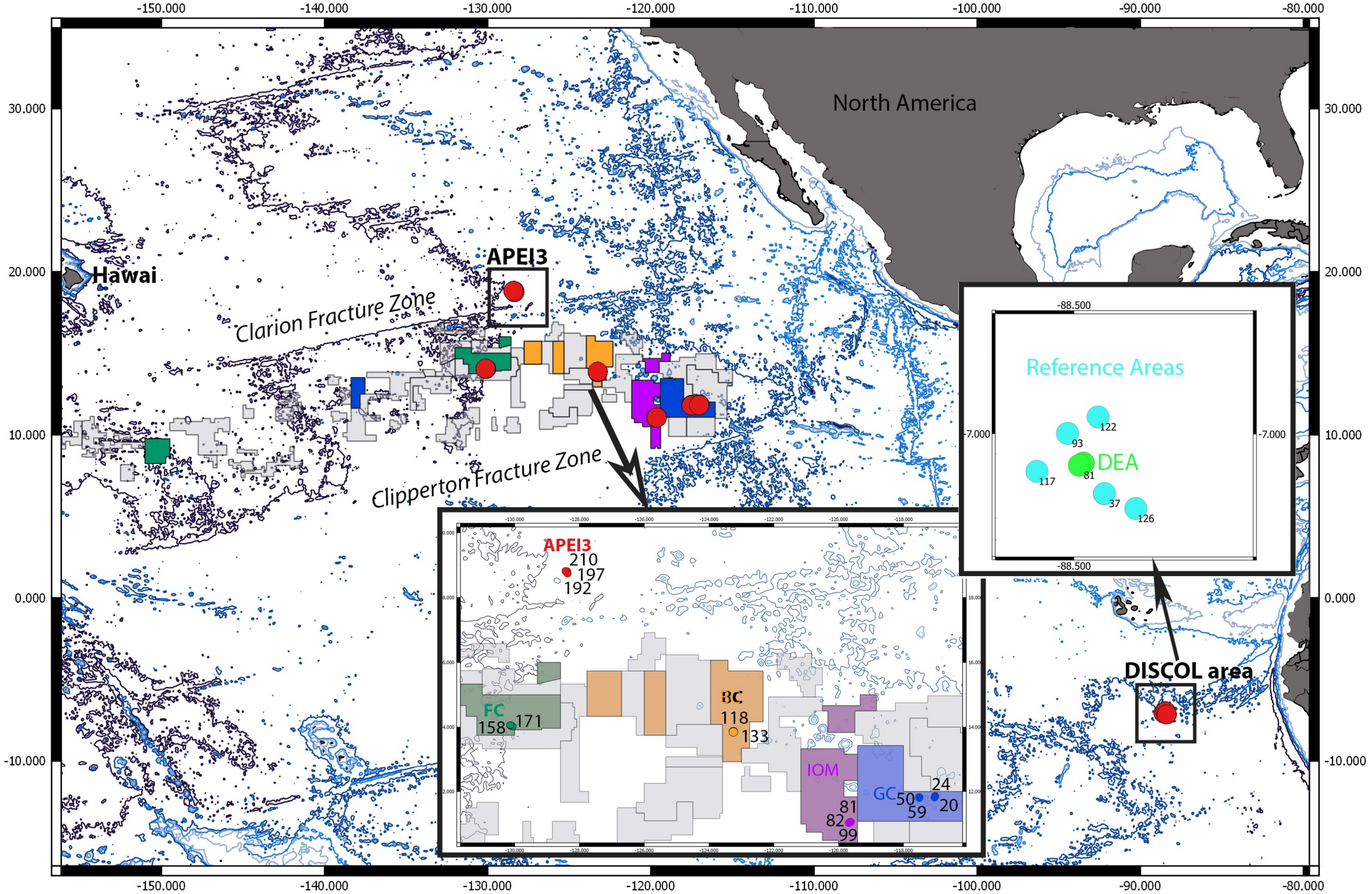
North America
Hawai
APEI3
Clarion Fracture Zone
Clipperton Fracture Zone
DISCOL area
Reference Areas
DEA
122
93
81
117
37
126
-88.500
-7.000
APEI3
210
197
192
FC
158
171
BC
118
133
IOM
GC
24
50
59
20
81
82
99
-150.000
-140.000
-130.000
-120.000
-110.000
-100.000
-90.000
-80.000
30.000
20.000
10.000
0.000
-10.000

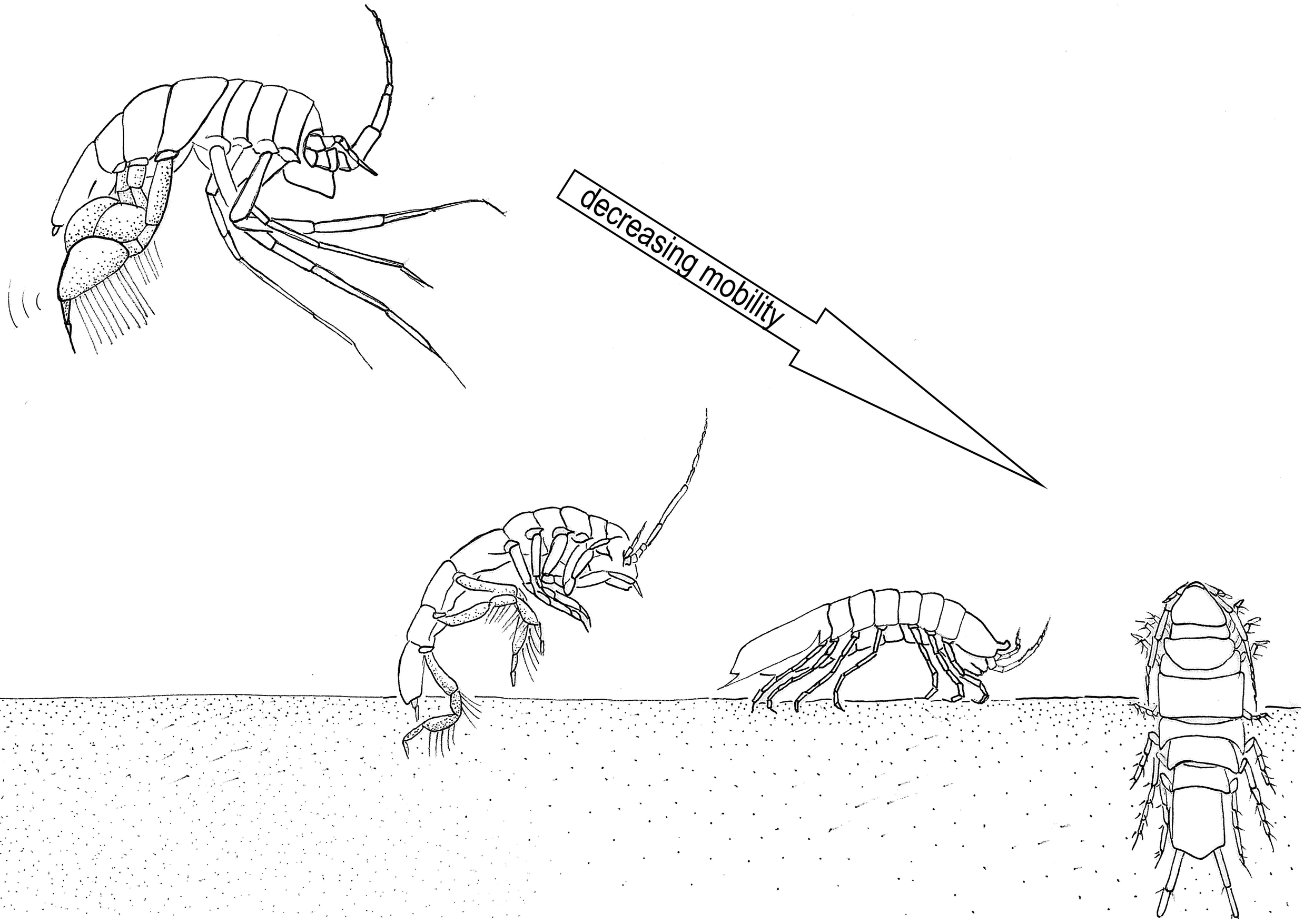
decreasing mobility

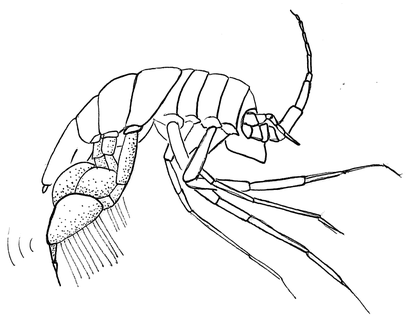

APEI3
BGR
IOM
GSR
IFREMER
DISCOL

0.4

Conserv.
Congruent

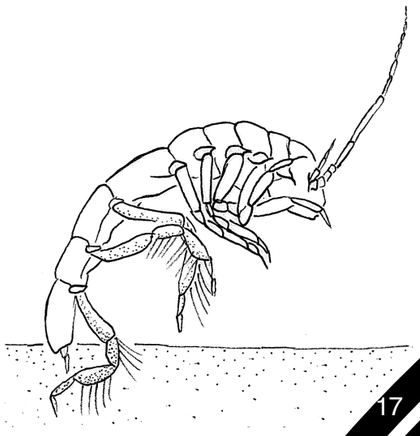

APEI3
BGR
IOM
GSR
IFREMER
DISCOL

DesmJP064_*Chelator_DisparellaUncertain*_IOM
DesmJP077_*PDisparella*_BC
DesmJP103_*Disparella*__FC
DesmJP075_cf_*Disparella*__BC
DesmJP148_cf_*Disparella*__A3
DesmJP140_*Chelator_DisparellaUncertain*_A3
DesmJP143_cf_*Disparella*__A3
DesmJP093_cf Disparella_sp1_BC
DesmJP021_*Disparella*_sp1_GC
DesmJP012_*Disparella*_sp1_GC
DesmJP013_cf_*Disparella*_sp1_GC
DesmDi30_Disparella_sp01_RHN
DesmJP125_*Disparella*__A3
DesmJP054_*Mirabilicoxa*_spC_IOM
DesmJP027_*Mirabilicoxa*_sp1_GC
DesmJP004_*Mirabilicoxa*_sp1_GC
DesmJP006_*Mirabilicoxa*_sp1_GC
DesmJP017_*Mirabilicoxa*_sp1_GC
DesmJP041_*Mirabilicoxa*_sp1_GC
DesmDi23_*Mirabilicoxa*_sp3_DEA
DesmDi08_*Mirabilicoxa*_sp3_RHN
DesmDi07_*Mirabilicoxa*_sp3_RS
DesmJP116_cf_*Mirabilicoxa*_spA_FC
DesmJP115_cf_*Mirabilicoxa*_spA_FC
DesmJP105_*Mirabilicoxa*_spA_FC
DesmJP111_*Mirabilicoxa*_spA_FC
DesmJP118_*Mirabilicoxa*_spA_FC
DesmJP073_*Mirabilicoxa*_spA_IOM
DesmJP121_*Prochelator*__FC
DesmJP082_*Prochelator*__BC
DesmDi11_*Prochelator*_sp01_RNw
DesmJP028_*Prochelator*_GC
DesmJP049_*Prochelator*_GC
DesmJP085_*Prochelator*_BC
DesmJP096_*Prochelator*_BC
DesmJP040_*Prochelator*_GC
DesmJP010_*Prochelator*_GC
DesmJP127_*Prochelator*_FC
DesmJP113_*Prochelator*_BC
DesmJP078_cf_*Prochelator*_BC
DesmJP086_*Prochelator*_BC
DesmJP087_*Prochelator*_BC
DesmJP088_*Prochelator*_BC
DesmJP123_*Prochelator*_FC
DesmDi28_Eugerdella_sp12_RHN
DesmJP126_*Eugerdella*_sp6Uncertain_A3
DesmJP147_*Eugerdella*_sp6Uncertain_A3
DesmJP162_*Eugerdella*_sp6Uncertain_A3
DesmJP051_cf_*Prochelator*_IOM
DesmJP068_*Eugerdella*_sp6_IOM
DesmJP057_*Eugerdella*_5or6_IOM
DesmJP065_*Eugerdella*_sp5_IOM
DesmJP055_cf_*Eugerdella*_IOM
DesmJP104_*Mirabilicoxa*_FC
DesmJP109_*Eugerdella*_sp6_FC
DesmJP142_*Eugerdella*_sp6Uncertain_A3
DesmJP042_*Eugerdella*_sp10_GC
DesmJP046_*Eugerdella*_sp10_GC
DesmJP043_*Eugerdella*_sp10_GC
DesmJP081_*Eugerdella*_sp10_BC
DesmJP008_Eugerdella_GC
DesmJP001_Eugerdella_sp11_GC
DesmJP019_Eugerdella_sp11_GC
DesmJP069_Eugerdella_sp11_IOM
DesmJP023_Eugerdella_sp11_GC
DesmJP059_Eugerdella_sp11_IOM
DesmJP039_Eugerdella_s11_GC
DesmJP016_Eugerdella_sp11_GC
DesmJP009_Eugerdella__GC
DesmJP024_Eugerdella_sp11_GC
DesmJP101_Eugerdella_sp8_FC
DesmJP007_Eugerdella_sp9_GC
DesmJP005_Eugerdella_sp9_GC
DesmJP071_Eugerdella_sp3_IOM
DesmJP076_Eugerdella_spcf7_BC
DesmJP110_Eugerdella_sp7_FC
DesmJP084_Eugerdella_sp5_BC
DesmJP053_Eugerdella_sp5_IOM
DesmJP117_Eugerdella_sp5_FC
DesmJP094_Eugerdella_sp5_BC
DesmJP120_Eugerdella_sp5_FC
DesmJP095_Eugerdella_sp5_BC
DesmJP112_Eugerdella_sp5_FC
DesmJP022_cf_Eugerdella_sp2_GC
DesmJP074_Eugerdella_cfegoni_BC
DesmJP092_Eugerdella_cfegoni_GC
DesmJP031_Eugerdella_BC
DesmJP037_Eugerdella_sp01_RHN
DesmDi31_Eugerda_sp01_DEA
DesmDi09_Eugerda_sp01_RS
DesmDi03 Eugerdella/Eugerda indet RS
DesmDi02 Eu / Des? sp03 RS
EF682292_*Betamorpha_africana*_G6
Ef116524_*Betamorpha_fusiformis*_BF7
Ef116525_*Betamorpha_fusiformis*_BF9
Ef116528_*Betamorpha_fusiformis*_BF12
Ef116527_*Betamorpha_fusiformis*_BF11
DesmJP138_*Chelator*_spA_A3
DesmJP139_*Chelator*_spA_A3
DesmJP145_cf_*Chelator*_spA_A3
DesmJP133_*Chelator*_spA_A3
DesmDi12_*Chelator*_sp01_RNw
DesmJP119_*Chelator*_spB_FC
DesmJP159_cf_*Chelator*_spC_A3
DesmJP153_*Chelator*_spC_A3
DesmJP152_*Chelator*_spC_A3
DesmJP091_*Chelator*_spD_BC
DesmDi20_*Chelator*_sp02_Rwo
DesmJP061_*Chelator*_spD_IOM
DesmJP050_*Chelator*_spD_IOM
DesmJP060_*Chelator*_spD_IOM
DesmJP135_cf_*Oecidiobranchus*_*oeci*_A3
DesmJP154_cf_*Oecidiobranchus*_*oeci*_A3
DesmJP137_cf_*Oecidiobranchus*_*oeci*_A3
DesmJP020_*Mirabilicoxa*_spC_GC
DesmJP038_*Mirabilicoxa*_spC_GC
DesmJP048_cf_*Mirabilicoxa*_spC_GC
DesmJP002_*Mirabilicoxa*_spC_GC
DesmJP134_cf_*Mirabilicoxa*_spB_A3
DesmJP131_*Mirabilicoxa*_spB_A3
DesmJP107_cf_*Mirabilicoxa*_spB_FC
DesmJP128_cf_*Mirabilicoxa*_spB_A3
DesmJP099_*Mirabilicoxa*_spD_FC
DesmJP083_*Mirabilicoxa*_spD_BC
DesmJP011_*Mirabilicoxa*_spD_GC
DesmJP066_*Mirabilicoxa*_spD_IOM
DesmJP033_*Mirabilicoxa*_spD_GC
DesmJP108_cf_*Mirabilicoxa*_spE_FC
DesmJP114_cf_*Mirabilicoxa*_spE_FC
DesmJP106_*Mirabilicoxa*_spE_FC
DesmJP100_*Mirabilicoxa*_spE_FC
DesmJP015_*Mirabilicoxa*_spF_GC
DesmJP025_*Mirabilicoxa*_spF_GC
DesmJP032_*Mirabilicoxa*_spF_GC
DesmJP067_*Mirabilicoxa*_IOM
DesmJP018_cf_*Mirabilicoxa*_GC
DesmDi24_*Mirabilicoxa*_sp01_Rwo
DesmDi21_*Mirabilicoxa*_sp01_RNw
DesmJP160_*Mirabilicoxa*_indet_A3
DesmJP129_*Mirabilicoxa*_A3
DesmJP124_*Mirabilicoxa*_A3
DesmJP045_*Eugerdella*_sp3_GC
DesmJP030_*Eugerdella*_sp4_GC
DesmJP026_*Eugerdella*_sp3_GC
DesmDi17_*Eugerdella*_sp01_RNw
DesmJP034_*Eugerdella*_sp3_GC
DesmJP047_*Eugerdella*_sp3_GC

0.3

Conservative
Congruent

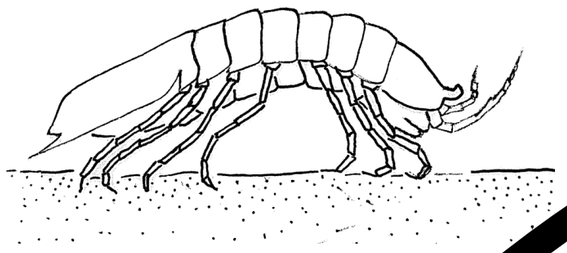

APEI3
BGR
IOM
GSR
IFREMER
DISCOL

HaplJP071_*Haploniscus*_sp2_A3
HaplJP062_*Haploniscus*_sp2_A3
HaplJP065_*Haploniscus*_sp2_A3
HaplJP060_*Haploniscus*_sp2_A3
HaplJP058_*Haploniscus*_sp2_A3
HaplJP067_*Haploniscus*_sp2_A3
HaplJP070_*Haploniscus*_sp2_FC
HaplJP054_*Haploniscus*_sp2_FC
HaplJP049_*Haploniscus*_sp2_FC
HaplJP050_*Haploniscus*_sp2_FC
HaplJP043_*Haploniscus*_sp2_FC
HaplJP019_*Haploniscus*_sp2_IOM
HaplJP032_*Haploniscus*_sp2_BC
HaplJP033_*Haploniscus*_sp2_BC
HaplJP016_*Haploniscus*_sp2_GC
HaplJP013_*Haploniscus*_sp2_GC
HaplJP015_*Haploniscus*_sp2_GC
HaplJP010_*Haploniscus*_sp2_GC
HaplJP014_*Haploniscus*_sp2_GC
HaplJP022_*Haploniscus*_sp2_IOM
HaplDi24_*Chauliodoniscus*_sp01_RNw
HaplJP003_*Haploniscus*_sp2_GC
HaplJP006_*Haploniscus*_sp2_GC
HaplJP061_*Mastigoniscus*_sp5_A3
HaplJP059_*Haploniscus*_sp5_A3
HaplJP020_*Haploniscus*_sp5_IOM
HaplJP064_*Mastigoniscus*_sp5_A3
HaplDi05_cf_*Chauliodoniscus*_nov._sp._01_RNw
HaplDi19_cf_*Chauliodoniscus*_DEA
HaplDi16_cf_*Chauliodoniscus*_nov._sp._01_RNw
HaplDi12_cf_*Chauliodoniscus*_nov._sp._01_RNw
HaplDi14_cf_*Chauliodoniscus*_nov._sp._01_RNw
HaplJP008_*Haploniscus*_sp4_GC
HaplJP045_*Haploniscus*_sp1_FC
HaplJP046_*Haploniscus*_sp1_FC
HaplJP044_*Haploniscus*_sp1a_FC
HaplJP052_*Haploniscus*_sp1_FC
HaplJP055_*Haploniscus*_sp1_FC
HaplJP057_*Mastigoniscus*_sp8_A3
HaplJP072_*Mastigoniscus*_sp8_A3
HaplJP063_*Mastigoniscus*_sp3_A3
HaplJP066_*Mastigoniscus*_sp3_A3
*laniropsis_epilittoralis*_2
*laniropsis_epilittoralis*_1
HaplJP074_*Mastigoniscus*_sp3_IOM
HaplJP021_*Mastigoniscus*_sp3_IOM
HaplJP031_*Mastigoniscus*_sp3_BC
HaplJP023_*Mastigoniscus*_sp3_BC
HaplJP040_*Mastigoniscus*_sp3_BC
HaplJP036_*Mastigoniscus*_sp_BC
HaplJP034_*Mastigoniscus*_sp3_BC
HaplJP028_*Mastigoniscus*_sp3_BC
HaplJP035_*Mastigoniscus*_sp3_BC
HaplJP037_*Mastigoniscus*_sp3_BC
HaplJP025_*Mastigoniscus*_sp3_BC
HaplJP026_*Mastigoniscus*_sp3_BC
HaplDi15_*Chauliodoniscus*_sp01_RNw
HaplDi09_*Chauliodoniscus*_sp01_RNw
HaplJP041_*Mastigoniscus*_sp_nov3_BIONOD_FC
HaplJP048_*Mastigoniscus*_sp3_FC
HaplJP051_*Mastigoniscus*_sp3_FC
HaplJP068_*Mastigoniscus*_sp5_A3
HaplJP069_*Mastigoniscus*_sp5_A3
HaplJP073_*Haploniscus*_sp5_A3
HaplJP024_*Mastigoniscus*_sp3007_BC
HaplJP029_*Mastigoniscus*_sp3007_BC
HaplJP038_*Mastigoniscus*_sp3007_BC
HaplJP027_*Mastigoniscus*_sp3007_BC
HaplJP039_*Mastigoniscus*_sp3007_BC
HaplJP042_*Mastigoniscus*_sp3007_FC
HaplJP002_*Mastigoniscus*_sp3Brokeland_GC
HaplJP004_*Mastigoniscus*_sp3Brokeland_GC
HaplJP009_*Mastigoniscus*_sp3Brokeland_GC
HaplJP005_*Mastigoniscus*_sp3Brokeland_GC
HaplJP001_*Mastigoniscus*_sp5_GC
HaplJP011_*Mastigoniscus*_sp5_IOM
HaplJP018_*Mastigoniscus*_sp5_GC
HaplJP017_*Mastigoniscus*_sp5_GC
HaplDi13_*Chauliodoniscus*_sp01_RNw
HaplDi02_*Chauliodobiscus*_sp01_RNw
HaplDi03_*Chauliodobiscus*_sp01_RNw
HaplDi04_*Chauliodoniscus*_sp01_RNw
HaplDi11_*Chauliodoniscus*_sp01_RNw
HaplDi17_*Chauliodoniscus*_sp01_RNw
HaplDi07_*Chauliodoniscus*_sp01_RNw
HaplDi08_*Chauliodoniscus*_sp01_RNw
HaplDi18_*Chauliodoniscus*_sp01_RNw
HaplJP053_*Haploniscus*_sp7_FC
HaplJP047_*Haploniscus*_sp7_FC

0.2

Conservative
Congruent

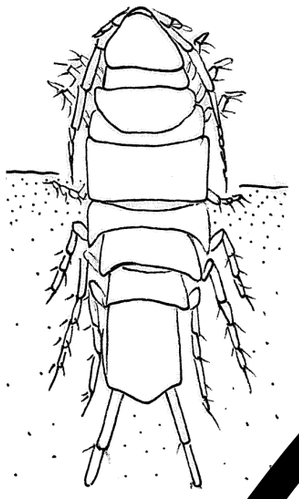

APEI3
BGR
IOM
GSR
IFREMER
DISCOL

MacrJP063_Macrostylis_spM_FC
MacrJP070_Macrostylis_spM_FC
MacrJP068_Macrostylis_spM_FC
MacrJP059_Macrostylis_spM_FC
MacrJP064_Macrostylis_spM_FC
MacrJP058_Macrostylis_spM_FC
MacrJP066_Macrostylis_spM_FC
MacrJP065_Macrostylis_spM_FC
MacrJP071_Macrostylis_spM_FC
MacrJP073_Macrostylis_spM_A3
MacrJP069_Macrostylis_spM_FC
MacrJP036_Macrostylis_spM_IOM
MacrJP041_Macrostylis_spM_IOM
MacrJP042_Macrostylis_spM_IOM
MacrJP039_Macrostylis_spM_IOM
MacrJP040_Macrostylis_spM_IOM
MacrJP052_Macrostylis_spM_BC
MacrJP044_Macrostylis_spM_BC
MacrJP048_Macrostylis_spM_BC
MacrJP049_Macrostylis_spM_BC
MacrJP043_Macrostylis_spM_BC
MacrJP045_Macrostylis_spM_BC
MacrJP026_Macrostylis_spM_GC
MacrJP030_Macrostylis_spM_GC
MacrJP031_Macrostylis_spM_GC
MacrJP028_Macrostylis_spM_GC
MacrJP034_Macrostylis_spM_GC
MacrJP032_Macrostylis_spM_GC
MacrJP027_Macrostylis_spM_GC
MacrJP033_Macrostylis_spM_GC
MacrJP046_Macrostylis_spM_BC
MacrJP047_Macrostylis_spM_BC
MacrJP083_Macrostylis_sp2_A3
MacrJP091_Macrostylis_sp2_A3
MacrJP074_Macrostylis_sp2_A3
MacrJP087_Macrostylis_sp2_A3
MacrJP085_Macrostylis_sp2_A3
MacrJP088_Macrostylis_sp3_A3
MacrJP086_Macrostylis_sp2_A3
MacrJP084_Macrostylis_sp2_A3
MacrJP005_Macrostylis_sp1_GC
MacrJP017_Macrostylis_sp1_GC
MacrJP016_Macrostylis_cfsp1_GC
MacrJP010_Macrostylis_spM_GC
MacrJP038_Macrostylis_cfsp1_IOM
KY951731_Thaumastosoma_diva_D3D64
Thaumastosoma_platycarpus_IDesm10
KM14_Iso261_Ketosoma_sp._2
KY951729_Ketosoma_hessleri_VT569
Ketosoma_vemae_VTDes013
MacrDi09_Macrostylis_sp03_FNw
MacrDi08_Macrostylis_sp03_DEA
MacrDi04_Macrostylis_sp03_RS
MacrDi07_Macrostylis_sp03_DEA
MacrJP062_Macrostylis_spM_FC
MacrJP050_Macrostylis_spM_BC
MacrJP054_Macrostylis_spM_BC
MacrJP053_Macrostylis_spM_BC
MacrJP055_Macrostylis_spM_FC
MacrJP061_Macrostylis_spM_FC
MacrJP067_Macrostylis_spM_FC
MacrJP060_Macrostylis_spM_FC
MacrJP057_Macrostylis_spM_FC
MacrJP072_Macrostylis_spM_FC
MacrJP090_Macrostylis_spM_A3
MacrJP078_Macrostylis_spM_A3
MacrJP077_Macrostylis_spM_A3
MacrJP080_Macrostylis_spM_A3
MacrJP079_Macrostylis_spM_A3
MacrJP082_Macrostylis_spM_A3
MacrJP081_Macrostylis_spM_A3
MacrJP089_Macrostylis_spM_A3
MacrJP075_Macrostylis_spM_A3
MacrJP076_Macrostylis_spM_A3
MacrJP023_Macrostylis_spM_GC
MacrJP014_Macrostylis_spM_GC
MacrJP035_Macrostylis_spM_IOM
MacrJP037_Macrostylis_spM_IOM
MacrJP022_Macrostylis_spM_GC
MacrJP021_Macrostylis_spM_GC
MacrJP025_Macrostylis_spM_GC
MacrJP024_Macrostylis_spM_GC
MacrJP029_Macrostylis_spM_GC
MacrJP013_Macrostylis_spM_GC
MacrJP020_Macrostylis_spM_GC
MacrJP009_Macrostylis_spM_GC
MacrJP019_Macrostylis_spM_GC
MacrJP015_Macrostylis_spM_GC
MacrJP011_Macrostylis_spM_GC
MacrJP001_Macrostylis_spM_GC
MacrJP002_Macrostylis_spM_GC
MacrJP018_Macrostylis_spM_GC
MacrJP003_Macrostylis_spM_GC
MacrJP007_Macrostylis_spM_GC
MacrJP012_Macrostylis_spM_GC
MacrJP004_Macrostylis_spM_GC
MacrJP006_Macrostylis_spM_GC
MacrJP008_Macrostylis_spM_GC

0.2

Conservative
Congruent

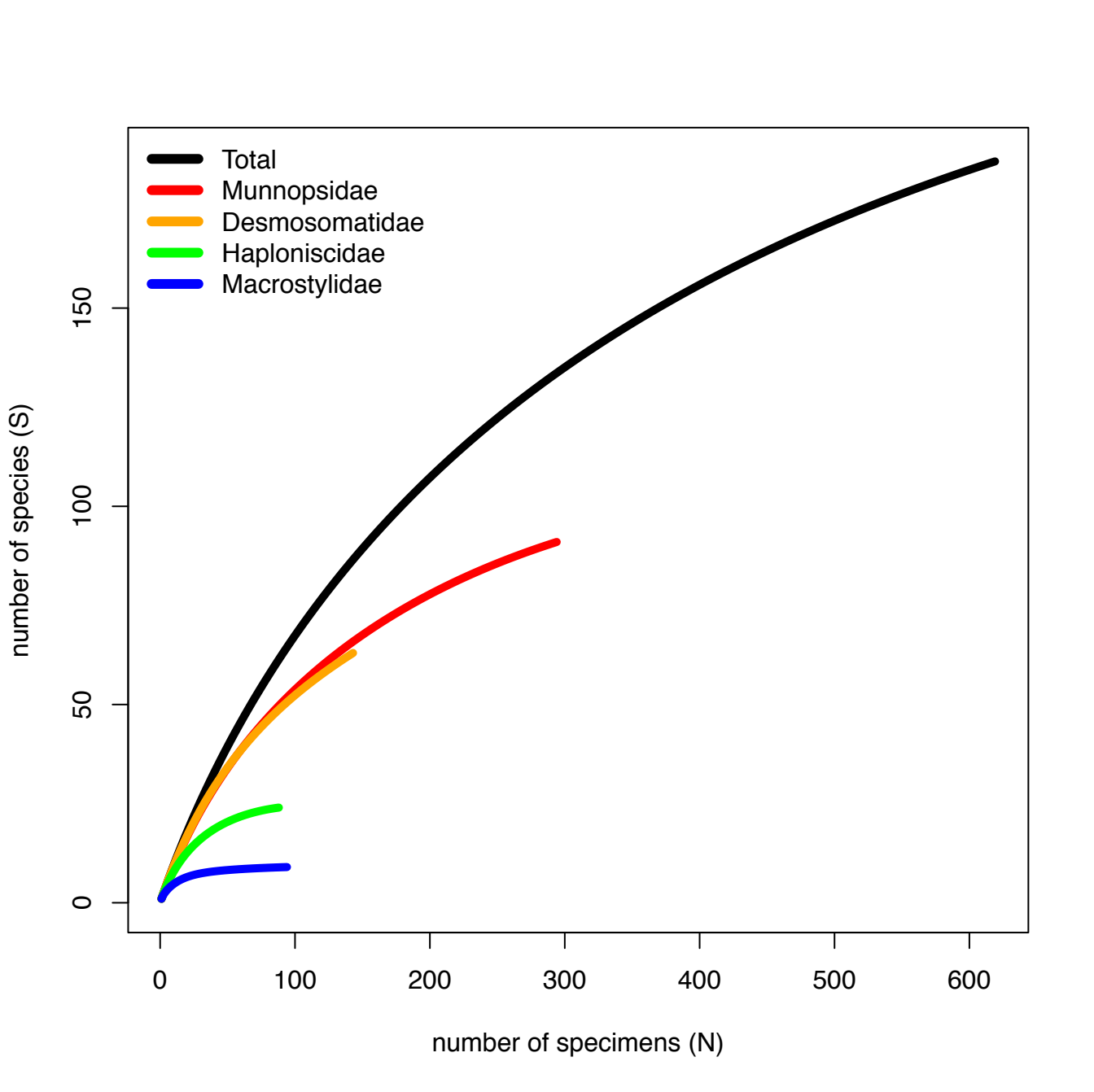
Total
Munnopsidae
Desmosomatidae
Haploniscidae
Macrostylidae
number of species (S)
0
50
100
150
0
100
200
300
400
500
600
number of specimens (N)

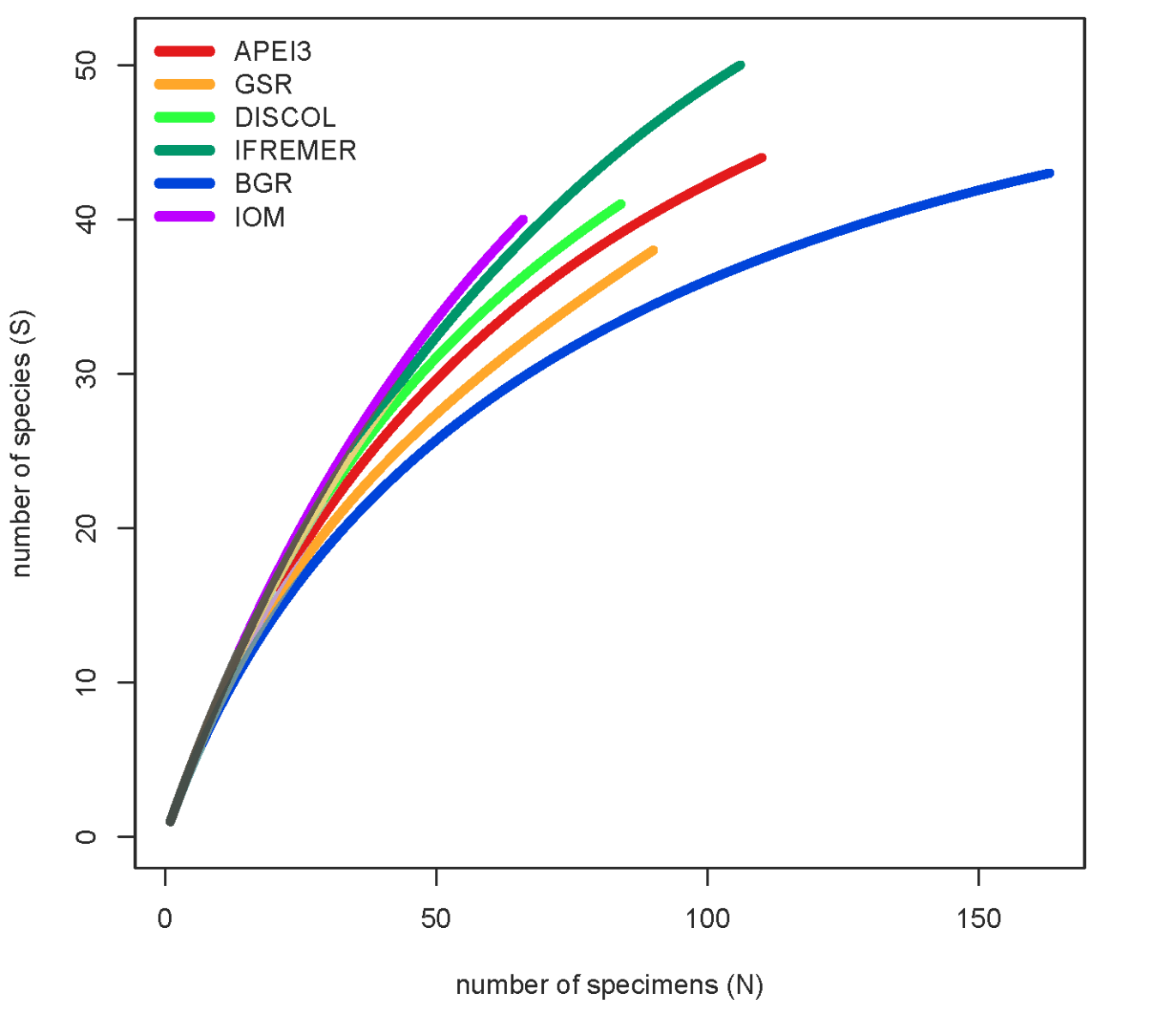
APEI3
GSR
DISCOL
IFREMER
BGR
IOM
number of species (S)
0
10
20
30
40
50
0
50
100
150
number of specimens (N)

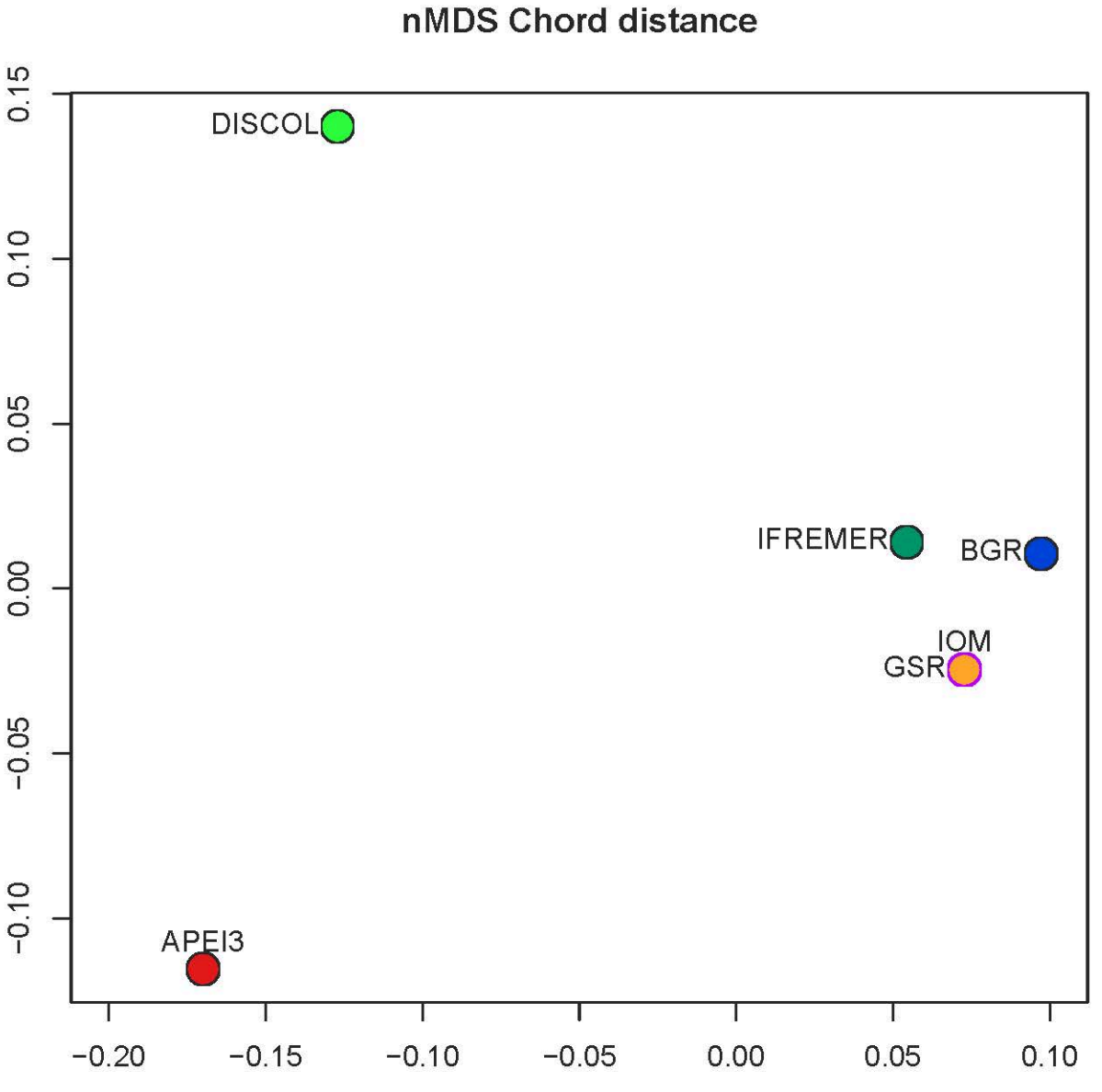
nMDS Chord distance
DISCOL
IFREMER
BGR
IOM
GSR
APEI3
0.15
0.10
0.05
0.00
−0.05
−0.10
−0.20
−0.15
−0.10
−0.05
0.00
0.05
0.10

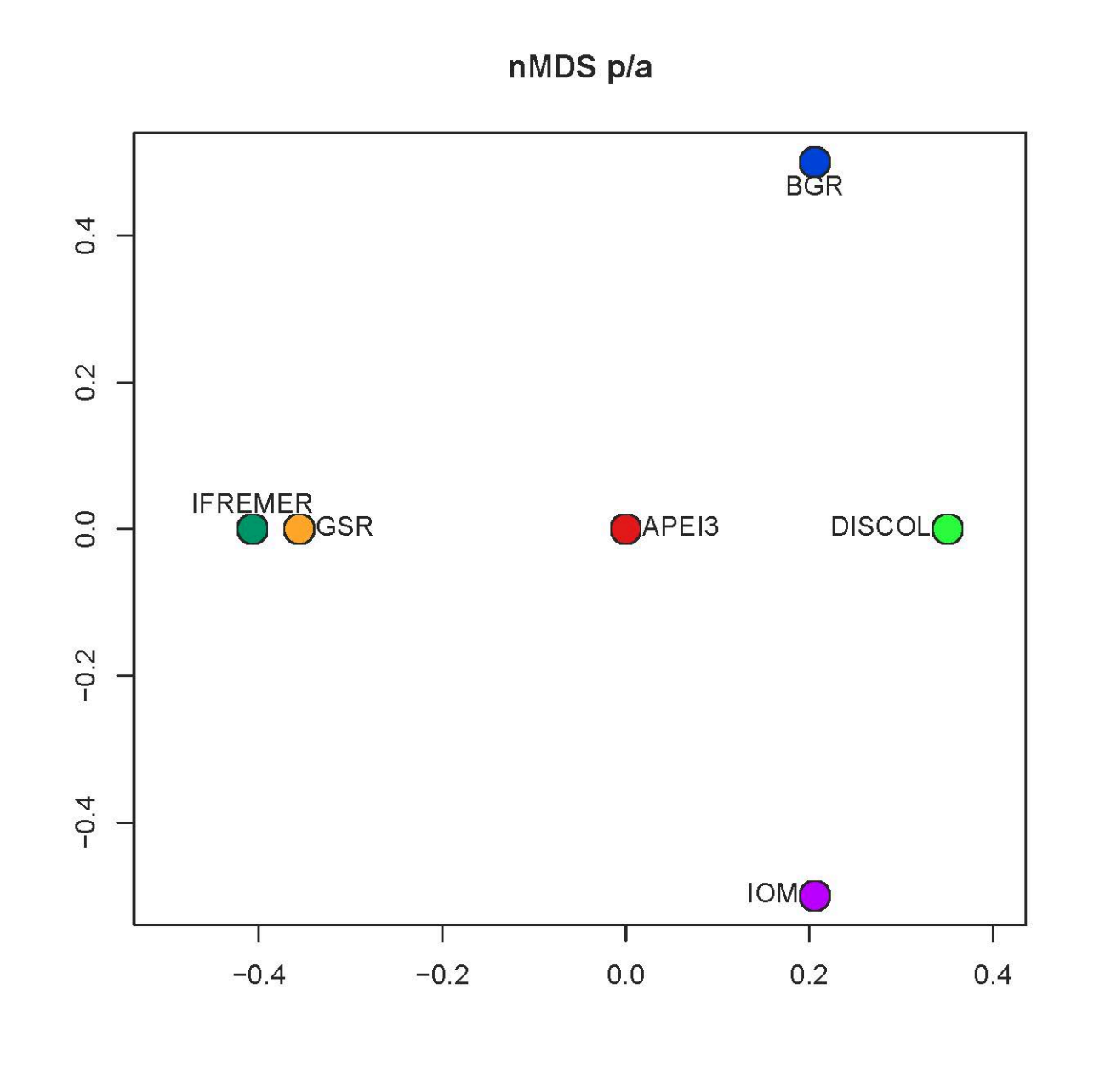
nMDS p/a
BGR
IFREMER
GSR
APEI3
DISCOL
IOM
0.4
0.2
0.0
−0.2
−0.4
−0.4
−0.2
0.0
0.2
0.4

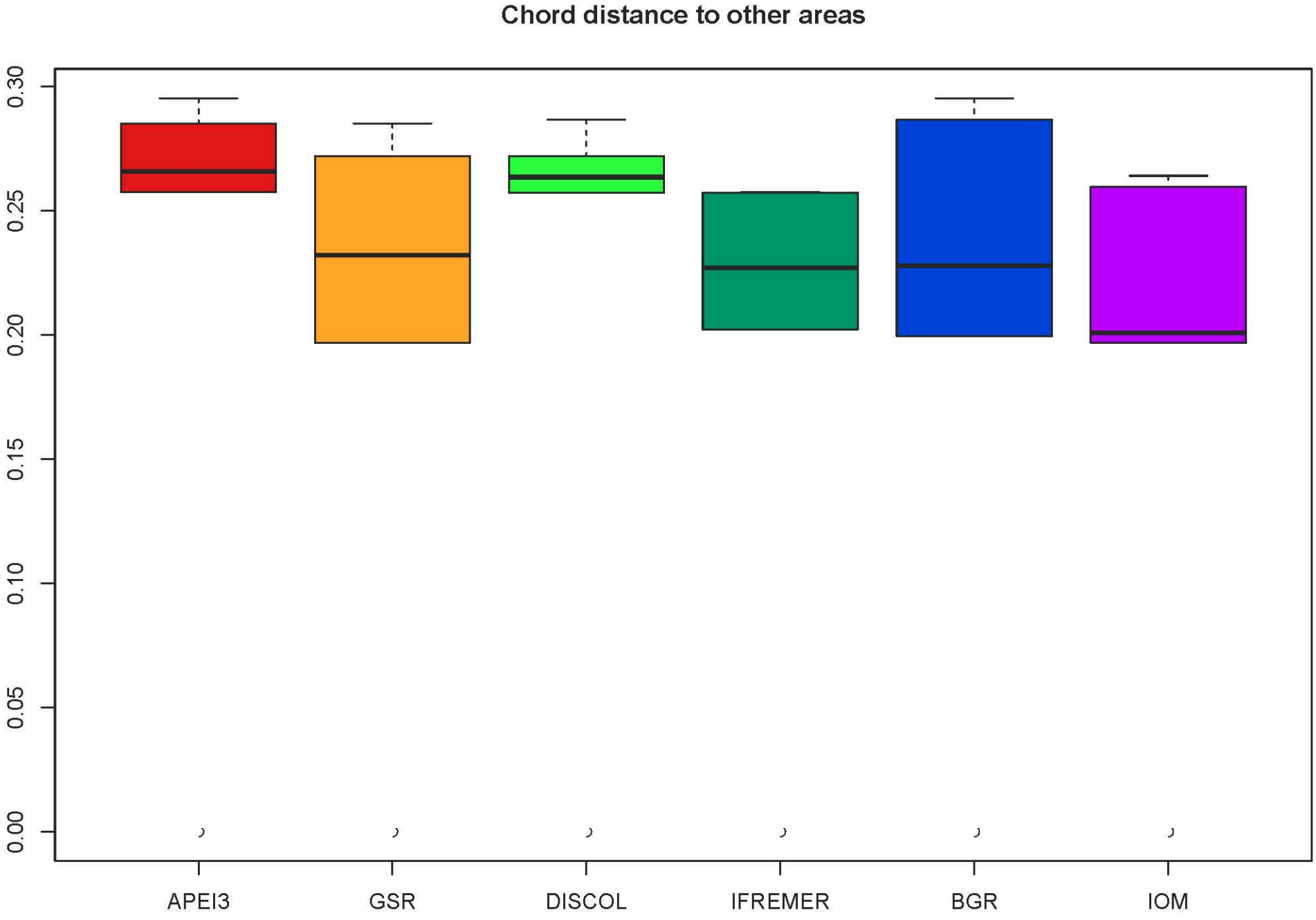
Chord distance to other areas
0.00
0.05
0.10
0.15
0.20
0.25
0.30
APEI3
GSR
DISCOL
IFREMER
BGR
IOM

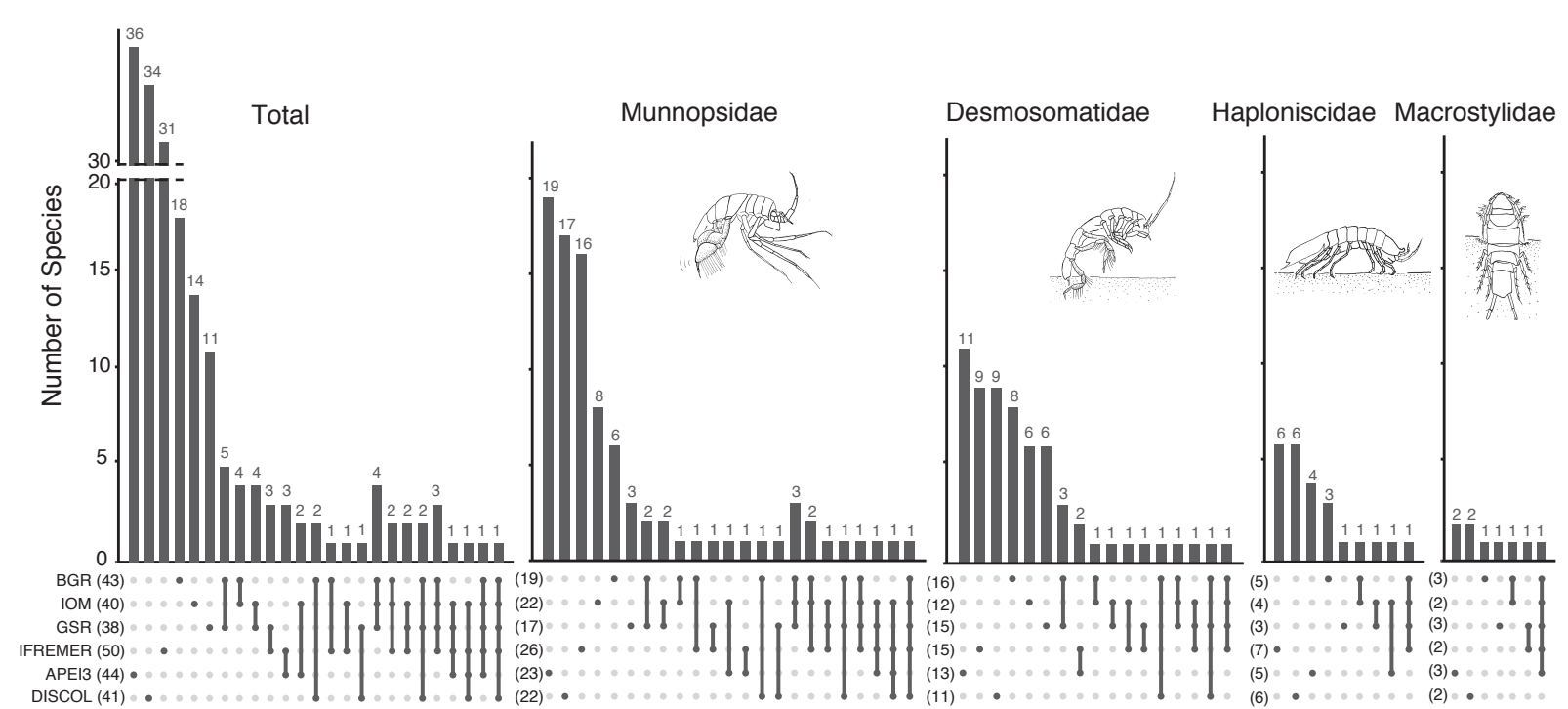
Number of Species
0
5
10
15
20
30
Total
36
34
31
18
14
11
5
4
4
3
3
2
2
1
1
1
4
2
2
2
3
1
1
1
1
Munnopsidae
19
17
16
8
6
3
2
2
1
1
1
1
1
1
1
3
2
1
1
1
1
1
1
Desmosomatidae
11
9
9
8
6
6
3
2
1
1
1
1
1
1
1
1
1
Haploniscidae
6
6
4
3
1
1
1
1
1
Macrostylidae
2
2
1
1
1
1
1
BGR (43)
IOM (40)
GSR (38)
IFREMER (50)
APEI3 (44)
DISCOL (41)
(19)
(22)
(17)
(26)
(23)
(22)
(16)
(12)
(15)
(15)
(13)
(11)
(5)
(4)
(3)
(7)
(5)
(6)
(3)
(2)
(3)
(2)
(3)
(2)